



X-ray Continuum Emission and Broad Iron Lines



Introduction

AGN have **power law continua**.

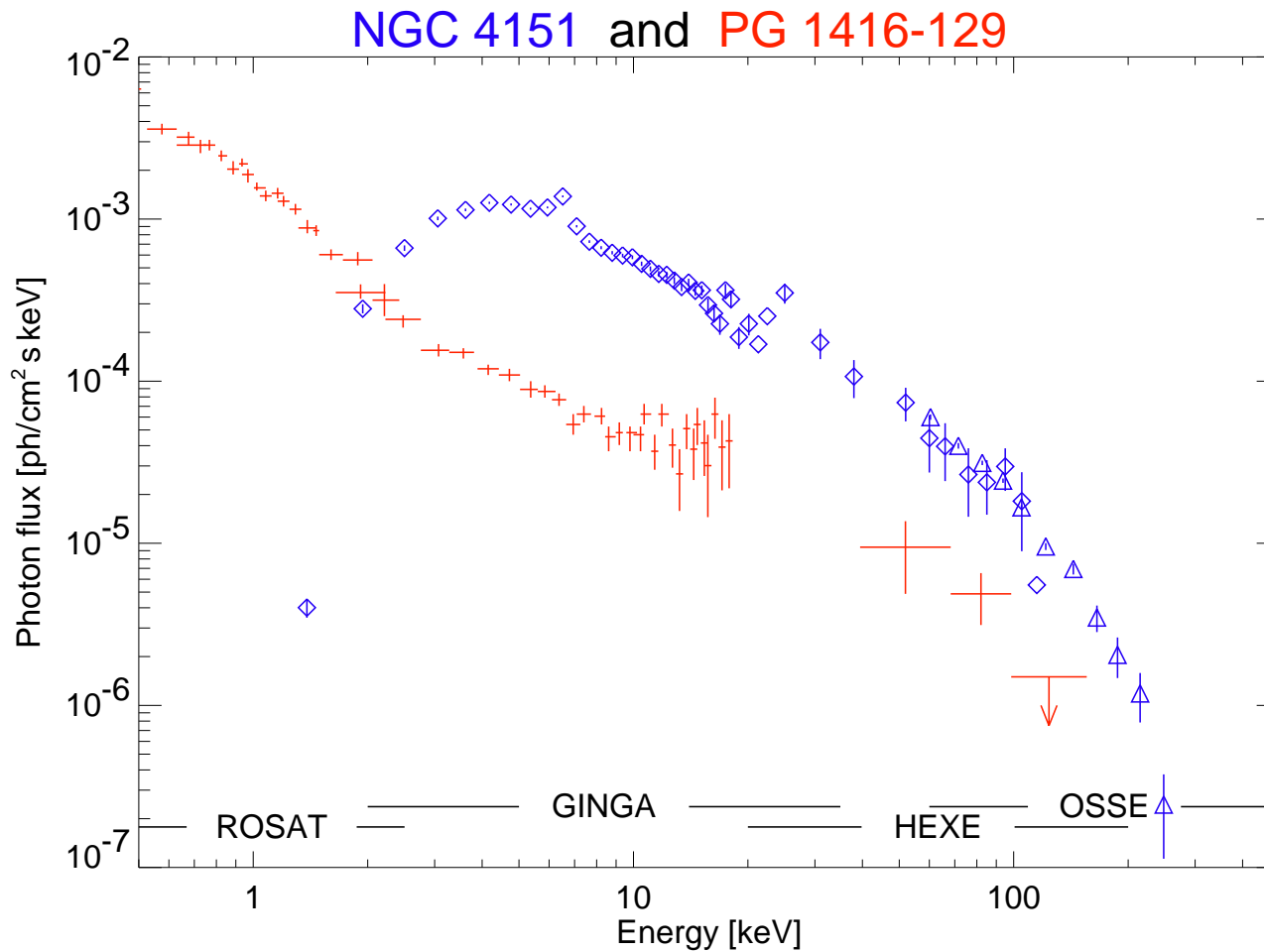
Purpose of this lecture: investigate physical origin of the continuum emission.

Structure:

1. **Compton Scattering** and **Comptonization**
2. Source of hot electrons
3. X-ray Reflection
4. Relativistic Broadened Fe $K\alpha$ Lines



AGN X-Ray Continua



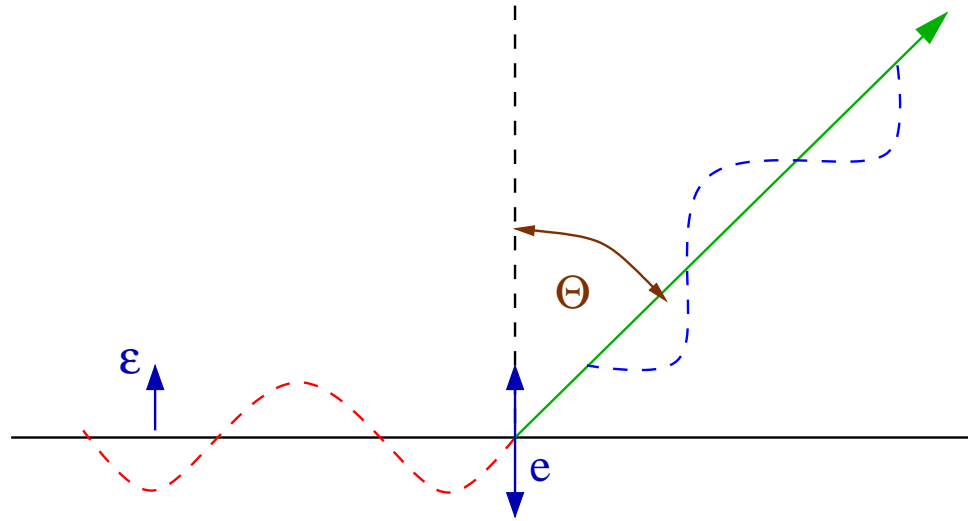
(PG 1416–129: de Kool et al., 1994, Williams et al., 1992, Staubert & Maisack, 1996; NGC 4151: Maisack 1991, 1993)

Note: NGC 4151 not corrected for interstellar absorption.

Spectral shape of AGN
very similar to galactic
Black Holes \implies Same
physical mechanism
(=Comptonization)
responsible!



Thomson Scattering, I



after Rybicki&Lightman, Fig. 3.6

Look at **radiation from free electron** in response to excitation of electron by an electromagnetic wave $E_0 \sin \omega_0 t$ (pointing in direction of unit-vector ϵ):

Force on charge

$$\mathbf{F} = m_e \dot{\mathbf{v}} = qE_0 \sin \omega_0 t \epsilon \quad (6.1)$$

This neglects the B -field, i.e., assumes $v \ll c$.

\implies The electron feels an acceleration, $\dot{\mathbf{v}}$, and therefore it radiates!



Thomson Scattering, II

The power radiated by an accelerated charge in direction Θ through the spherical angle $d\Omega$ is given by **Larmor's formula**:

$$\frac{dP}{d\Omega}(\Theta) = \frac{1}{16\pi^2 c^3 \epsilon_0} q^2 \dot{v}^2 \sin^2 \Theta \quad (6.2)$$

Integrating Eq. (6.2) over 4π sr gives

$$P = \frac{q^2 \dot{v}^2}{6\pi c^3 \epsilon_0} \quad (6.3)$$

For the case the charge is accelerated by an (sinusoidally varying) electric field $E(t)$ one finds after a longish calculation:

$$\frac{dP}{d\Omega} = \frac{q^4 E_0^2}{16\pi^2 m^2 c^3 \epsilon_0} \sin^2 \Theta \quad \text{and} \quad P = \frac{q^4 E_0^2}{12\pi c^3 m^2 \epsilon_0} \quad (6.4)$$



Thomson Scattering, III

The incident flux on the electron (i.e., $c \times$ energy density for radiation) is

$$\langle \mathbf{S} \rangle = \frac{c\epsilon_0}{2} E_0^2 \quad (6.5)$$

Define the **differential cross section** for Thomson scattering, $d\sigma/d\Omega$, such that

$$\frac{dP}{d\Omega} = \langle \mathbf{S} \rangle \frac{d\sigma}{d\Omega} \iff \frac{q^4 E_0^2}{16\pi^2 m^2 c^3 \epsilon_0} \sin^2 \Theta = \frac{c\epsilon_0^2}{2} E_0^2 \frac{d\sigma}{d\Omega} \quad (6.6)$$

such that

$$\left. \frac{d\sigma}{d\Omega} \right|_{\text{polarized}} = \frac{q^4}{8\pi^2 m^2 c^4 \epsilon_0^2} \sin^2 \Theta = r_0^2 \sin^2 \Theta \quad (6.7)$$

with the **classical electron radius**

$$r_0 = \frac{e^2}{4\pi m_e c^2 \epsilon_0} = 2.82 \times 10^{-15} \text{ m} \quad (6.8)$$



Thomson Scattering, IV

The **differential cross section** $d\sigma/d\Omega$ is the area presented by the electron to a photon that is going to get scattered in direction $d\Omega$.

The **total cross section** for Thomson scattering, σ_T , is then obtained from the differential cross section by integrating $d\sigma/d\Omega$ from Eq. (6.7) over all angles:

$$P = \int \langle S \rangle \frac{d\sigma}{d\Omega} d\Omega = \langle S \rangle \int \frac{d\sigma}{d\Omega} d\Omega =: \langle S \rangle \sigma_T \quad (6.9)$$

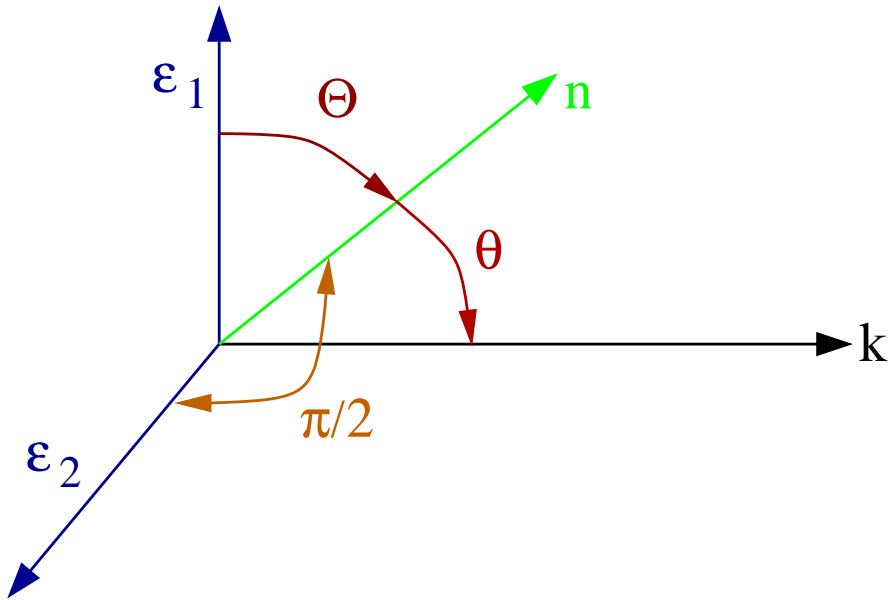
Performing the integration yields

$$\sigma_T = \frac{8\pi}{3} r_0^2 = \frac{e^4}{6\pi m_e^2 \epsilon_0^2 c^4} = 6.652 \times 10^{-25} \text{ cm}^2 \quad (6.10)$$

σ_T is also called the **Thomson cross section**.



Thomson Scattering, V



after Rybicki & Lightman, Fig. 3.7

For linear polarized light: **scattered radiation is linearly polarized** in direction of incident polarization vector, ϵ , and direction of scattering, \mathbf{n} .

To compute σ for **nonpolarized radiation**, note:
nonpolarized radiation = \sum polarized beams at

Thus, to scatter nonpolarized radiation propagating in direction \mathbf{k} into direction \mathbf{n} , need to average two scatterings:

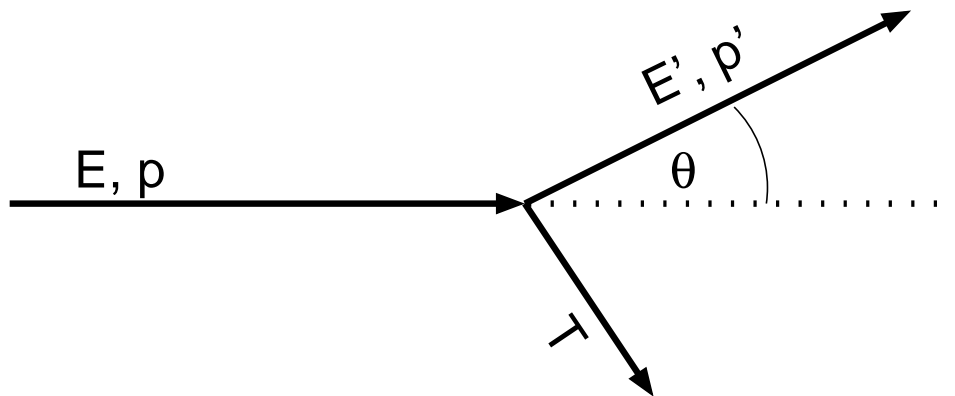
$$\left. \frac{d\sigma}{d\Omega} \right|_{\text{unpol}} = \frac{1}{2} \left(\left. \frac{d\sigma(\Theta)}{d\Omega} \right|_{\text{pol}} + \left. \frac{d\sigma(\pi/2)}{d\Omega} \right|_{\text{pol}} \right) \quad (6.11)$$

Let $\theta = \angle(\mathbf{k}, \mathbf{n})$ to obtain

$$\left. \frac{d\sigma}{d\Omega} \right|_{\text{unpol}} = \frac{r_0^2}{2} (1 + \cos^2 \theta) = \frac{3\sigma_T}{16\pi} (1 + \cos^2 \theta) \quad \text{and} \quad \int \frac{d\sigma}{d\Omega} d\Omega = \sigma_T \quad (6.12)$$



Compton Scattering



Thomson scattering: initial and final photon energy are identical.

But: in QM: light consists of photons

⇒ Scattering: photon changes direction

⇒ Momentum change

⇒ **Energy change!**

This process is called **Compton scattering**.

Energy/wavelength change in scattering (see handout):

$$E' = \frac{E}{1 + \frac{E}{m_e c^2} (1 - \cos \theta)} \sim E \left(1 - \frac{E}{m_e c^2} (1 - \cos \theta) \right) \quad (6.13)$$

$$\lambda' - \lambda = \frac{h}{m_e c} (1 - \cos \theta) \quad (6.14)$$

where $h/m_e c = 2.426 \times 10^{-12} \text{ m}$ (**Compton wavelength**).

Averaging over θ , for $E \ll m_e c$:

$$\frac{\Delta E}{E} \approx -\frac{E}{m_e c^2} \quad (6.15)$$

E.g., at 6.4 keV, $\Delta E \approx 0.2 \text{ keV}$.

The derivation of Eq. (6.13) is most simply done in special relativity using four-vectors. In the following, we will use capital letters for four-vectors and small letters for three-vectors. Furthermore, we will adopt the convention

$$\mathbf{P} \cdot \mathbf{Q} = P_0 Q_0 - P_1 Q_1 - P_2 Q_2 - P_3 Q_3 \quad (6.16)$$

for the product of two four vectors, following, e.g., the convention of Rindler (1991, Introduction to Special Relativity).

The four-momentum of a particle with non-zero rest-mass, m_0 , e.g., an electron, is

$$\mathbf{Q} = m_0 \gamma \begin{pmatrix} c \\ \mathbf{v} \end{pmatrix} = \begin{pmatrix} m_0 \gamma c \\ \mathbf{q} \end{pmatrix} \quad (6.17)$$

where \mathbf{v} is the velocity of the particle and \mathbf{q} its momentum. As usual, $\gamma = (1 - (v/c)^2)^{-1/2}$. The square of \mathbf{Q} is

$$\mathbf{Q}^2 = m_0^2 \gamma^2 c^2 - m_0^2 \gamma^2 v^2 = m_0^2 c^2 \gamma^2 \left(1 - \left(\frac{v^2}{c^2} \right) \right) = m_0^2 c^2 \quad (6.18)$$

Obviously, \mathbf{Q}^2 is relativistically invariant.

In the same spirit, the four-momentum of a photon is

$$\mathbf{P} = \frac{E}{c} \begin{pmatrix} 1 \\ \hat{\mathbf{u}} \end{pmatrix} \quad (6.19)$$

where $\hat{\mathbf{u}}$ is an unit-vector pointing into the direction of motion of the photon. Note that for photons

$$\mathbf{P}^2 = 0 \quad (6.20)$$

as the photon's rest-mass is zero.

We will now look at the collision between a photon and an electron. We will denote the four-momenta after the collision with primed quantities.

Conservation of four-momentum requires

$$\mathbf{P} + \mathbf{Q} = \mathbf{P}' + \mathbf{Q}' \quad (6.21)$$

We now use a trick from Lightman et al. (1975, Problem Book in Relativity and Gravitation), solving this equation for \mathbf{Q}' and squaring the resulting expression:

$$(\mathbf{P} + \mathbf{Q} - \mathbf{P}')^2 = (\mathbf{Q}')^2 \quad (6.22)$$

Since the collision is elastic, i.e., the rest mass of the electron is not changed by the collision,

$$\mathbf{Q}^2 = (\mathbf{Q}')^2 \quad (6.23)$$

furthermore, $\mathbf{P}^2 = (\mathbf{P}')^2 = 0$, such that

$$\mathbf{P} \cdot \mathbf{Q} - \mathbf{P} \cdot \mathbf{P}' - \mathbf{Q} \cdot \mathbf{P}' = 0 \quad \Leftrightarrow \quad \mathbf{P} \cdot \mathbf{P}' = \mathbf{Q} \cdot (\mathbf{P} - \mathbf{P}') \quad (6.24)$$

But in the frame where the electron is initially at rest,

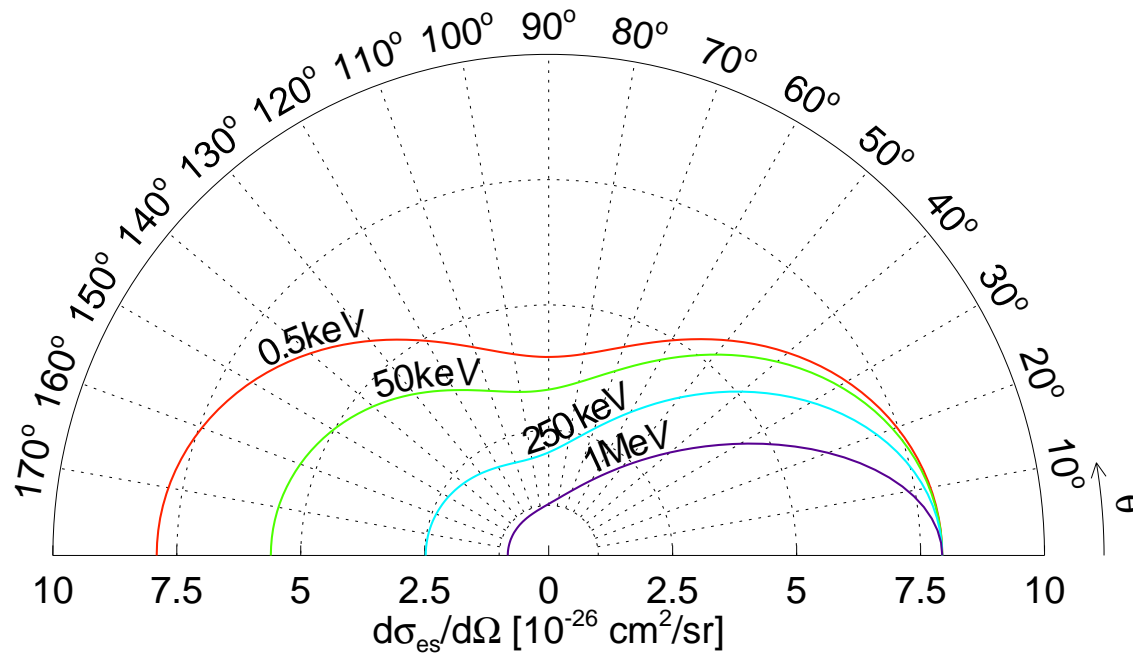
$$\mathbf{Q} \cdot (\mathbf{P} - \mathbf{P}') = m_e c \left(\frac{E}{c} - \frac{E'}{c} \right) = m(E - E') \quad (6.25)$$

$$\mathbf{P} \cdot \mathbf{P}' = \frac{E}{c} \frac{E'}{c} (1 - \hat{\mathbf{u}} \cdot \hat{\mathbf{u}}') = \frac{EE'}{c^2} (1 - \cos \theta) \quad (6.26)$$

where $\theta = \angle(\hat{\mathbf{u}}, \hat{\mathbf{u}}')$. Inserting into Eq. (6.24) and solving for E' gives Eq. (6.13).



Compton Scattering



The proper derivation of cross section is done in quantum electrodynamics.

In the limit of low energies: will find Thomson result, for higher energies: relativistic effects become important.

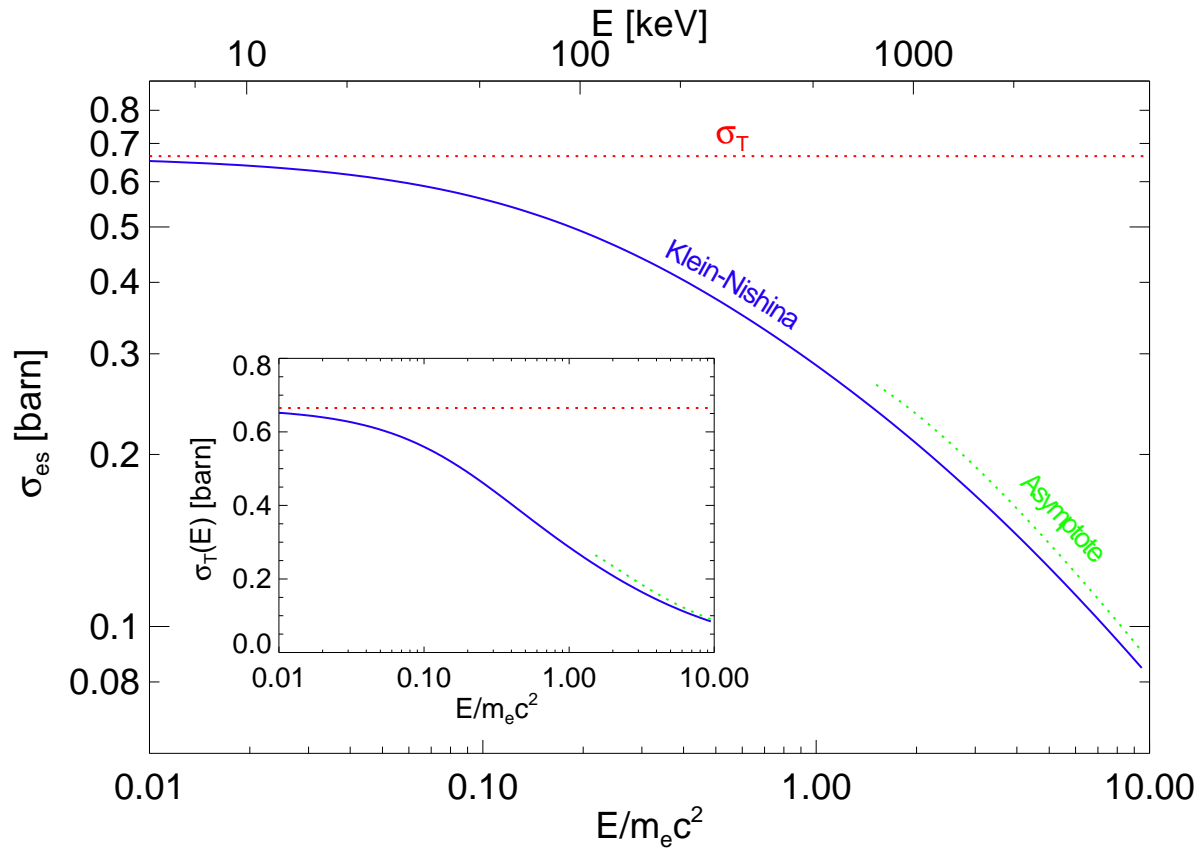
For **unpolarized radiation**,

$$\frac{d\sigma_{es}}{d\Omega} = \frac{3}{16\pi} \sigma_T \left(\frac{E'}{E} \right)^2 \left(\frac{E}{E'} + \frac{E'}{E} - \sin^2 \theta \right) \quad (6.27)$$

(Klein-Nishina formula).



Compton Scattering



1 barn = 10^{-28} m²

Integrating over $d\sigma_{es}/d\Omega$ gives total cross-section:

$$\sigma_{es} = \frac{3}{4}\sigma_T \left[\frac{1+x}{x^3} \left\{ \frac{2x(1+x)}{1+2x} - \ln(1+2x) \right\} + \frac{1}{2x} \ln(1+2x) - \frac{1+3x}{(1+2x)^2} \right] \quad (6.28)$$

where $x = E/m_e c^2$.



Energy Exchange

For **non-stationary** electrons, use previous formulae and Lorentz transform photon into electron's frame of rest (FoR):

1. **Lab system \Rightarrow electron's frame of rest:**

$$E_{\text{FoR}} = E_{\text{Lab}} \gamma (1 - \beta \cos \theta) \quad (6.29)$$

2. Scattering occurs, gives E'_{FoR} .

3. **Electron's frame of rest \Rightarrow Lab system:**

$$E'_{\text{Lab}} = E'_{\text{FoR}} \gamma (1 + \beta \cos \theta') \quad (6.30)$$

Therefore, if electron is relativistic:

$$E'_{\text{Lab}} \sim \gamma^2 E_{\text{Lab}} \quad (6.31)$$

since (on average) θ, θ' are $\mathcal{O}(\pi/2)$ (beaming!).

Thus: Energy transfer is **very** efficient.

As shown in the following, in Compton scattering the radiation field is also amplified by a factor γ^2 .

We first look at the energy budget of one single scattering.

The total power *emitted* in the frame of rest of the electron is given by

$$\left. \frac{dE'_{\text{FoR}}}{dt_{\text{FoR}}} \right|_{\text{em}} = \int c \sigma_{\text{T}} E'_{\text{FoR}} V'(E'_{\text{FoR}}) dE'_{\text{FoR}} \quad (6.32)$$

where $V'(E')$ is the **photon energy density distribution** (number of photons per cubic metre with an energy between E' and $E' + dE'$).

This power is **Lorentz invariant**:

$$\frac{V_{\text{Lab}}(E_{\text{Lab}}) dE_{\text{Lab}}}{E_{\text{Lab}}} = \frac{V_{\text{FoR}}(E_{\text{FoR}}) dE_{\text{FoR}}}{E_{\text{FoR}}} \quad (6.33)$$

In the ‘‘Thomson limit’’ one assumes that the energy change of the photon in the rest frame of the electron is small,

$$E'_{\text{FoR}} = E_{\text{FoR}} \quad (6.34)$$

(this limit was also used in the derivation of Eq. (6.31)). Furthermore one can show that the power is Lorentz invariant:

$$\frac{dE_{\text{FoR}}}{dt_{\text{FoR}}} = \frac{dE_{\text{Lab}}}{dt_{\text{Lab}}} \quad (6.35)$$

(this follows from the fact that energy and time are both ‘‘time-like quantities’’, i.e., the formulae for the Lorentz transform of energy and time are the same).

Therefore

$$\left. \frac{dE_{\text{Lab}}}{dt_{\text{Lab}}} \right|_{\text{em}} = c \sigma_{\text{T}} \int E_{\text{FoR}}^2 \frac{V_{\text{FoR}} dE_{\text{FoR}}}{E_{\text{FoR}}} \quad (6.36)$$

$$= c \sigma_{\text{T}} \int E_{\text{FoR}}^2 \frac{V_{\text{Lab}} dE_{\text{Lab}}}{E_{\text{Lab}}} \quad (6.37)$$

... Lorentz transforming E_{FoR}

$$= c \sigma_{\text{T}} \gamma^2 \int (1 - \beta \cos \theta)^2 E_{\text{Lab}} V_{\text{Lab}} dE_{\text{Lab}} \quad (6.38)$$

... averaging over angles ($\langle \cos \theta \rangle = 0$, $\langle \cos^2 \theta \rangle = \frac{1}{3}$)

$$= c \sigma_{\text{T}} \gamma^2 \left(1 + \frac{\beta^2}{3} \right) U_{\text{rad}} \quad (6.39)$$

6-12

where

$$U_{\text{rad}} = \int EV(E)dE \quad (6.40)$$

(initial photon energy density).

To determine the power gain of the photons, we need to subtract the power irradiated onto the electron,

$$\left. \frac{dE_{\text{Lab}}}{dt_{\text{Lab}}} \right|_{\text{inc}} = c\sigma_{\text{T}} \int EV(E)dE = \sigma_{\text{T}}cU_{\text{rad}} \quad (6.41)$$

Therefore, since

$$\gamma^2 - 1 = \gamma^2\beta^2 \quad (6.42)$$

the net power gain of the photon field is

$$P_{\text{compt}} = \left. \frac{dE_{\text{Lab}}}{dt} \right|_{\text{em}} - \left. \frac{dE_{\text{Lab}}}{dt} \right|_{\text{inc}} \quad (6.43)$$

$$= \frac{4}{3}\sigma_{\text{T}}c\gamma^2\beta^2U_{\text{rad}} \quad (6.44)$$



Amplification factor,

As shown before, in the electron frame of rest,

$$\frac{\Delta E}{E} = -\frac{E}{m_e c^2} \quad (6.15)$$

Assuming a thermal (Maxwell) distribution of electrons (i.e., they're not at rest), using the equations from the previous slides one can show that the relative energy change is given by

$$\frac{\Delta E}{E} = \frac{4kT - E}{m_e c^2} = A \quad (6.45)$$

where A is the **Compton amplification factor**.

Thus:

$E \lesssim 4kT_e \implies$ Photons gain energy, gas cools down.

$E \gtrsim 4kT_e \implies$ Photons lose energy, gas heats up.



Amplification factor, II

In reality, photons will scatter more than once before leaving the hot electron medium.

The *total* relative energy change of photons by traversal of a hot ($E \ll kT_e$) medium with electron density n_e and size ℓ is then approximately

$$(\text{rel. energy change } y) = \frac{\text{rel. energy change}}{\text{scattering}} \times (\# \text{ scatterings}) \quad (6.46)$$

The number of scatterings is $\max(\tau_e, \tau_e^2)$, where $\tau_e = n_e \sigma_T \ell$ (“**optical depth**”), such that

$$y = \frac{4kT_e}{m_e c^2} \max(\tau_e, \tau_e^2) \quad (6.47)$$

“Compton y -Parameter”



Spectral shape, I

Photon spectra can be found by analytically solving the “Kompaneets equation”, but this is very difficult.

Approximate spectral shape from the following arguments:

After k scatterings, the energy of a photon with initial energy E_i is approximately

$$E_k = E_i A^k \quad (6.48)$$

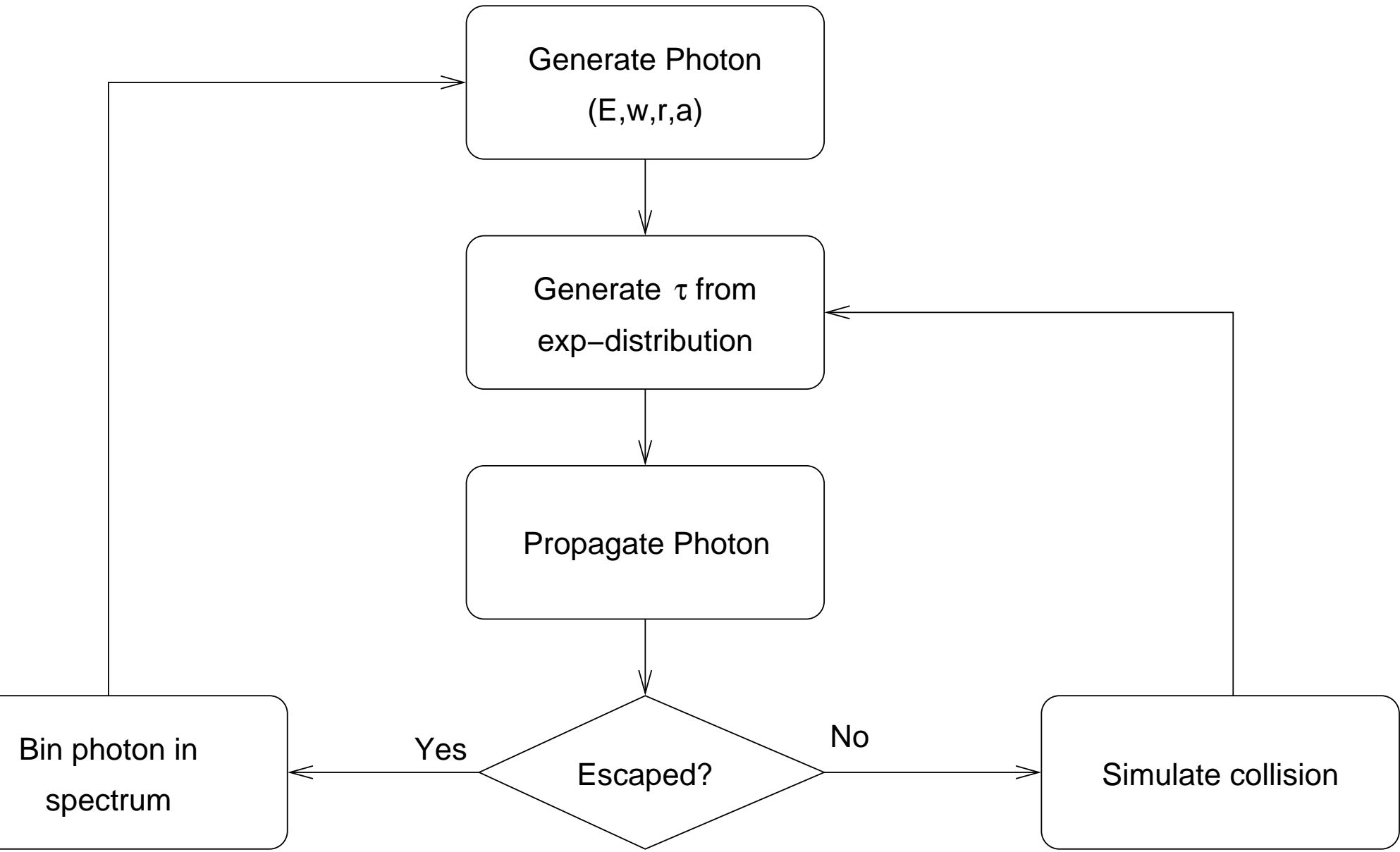
But the probability to undergo k scatterings in a cloud with optical depth τ_e is $p_k(\tau_e) = \tau_e^k$ (follows from theory of random walks, note that the mean free path is $\ell = 1/\tau_e$).

Therefore, if there are $N(E_i)$ photons initially, then the number of photons emerging at energy E_k is

$$N(E_k) \sim N(E_i) A^k \sim N(E_i) \left(\frac{E_k}{E_i} \right)^{-\alpha} \quad \text{with} \quad \alpha = -\frac{\ln \tau_e}{\ln A} \quad (6.49)$$

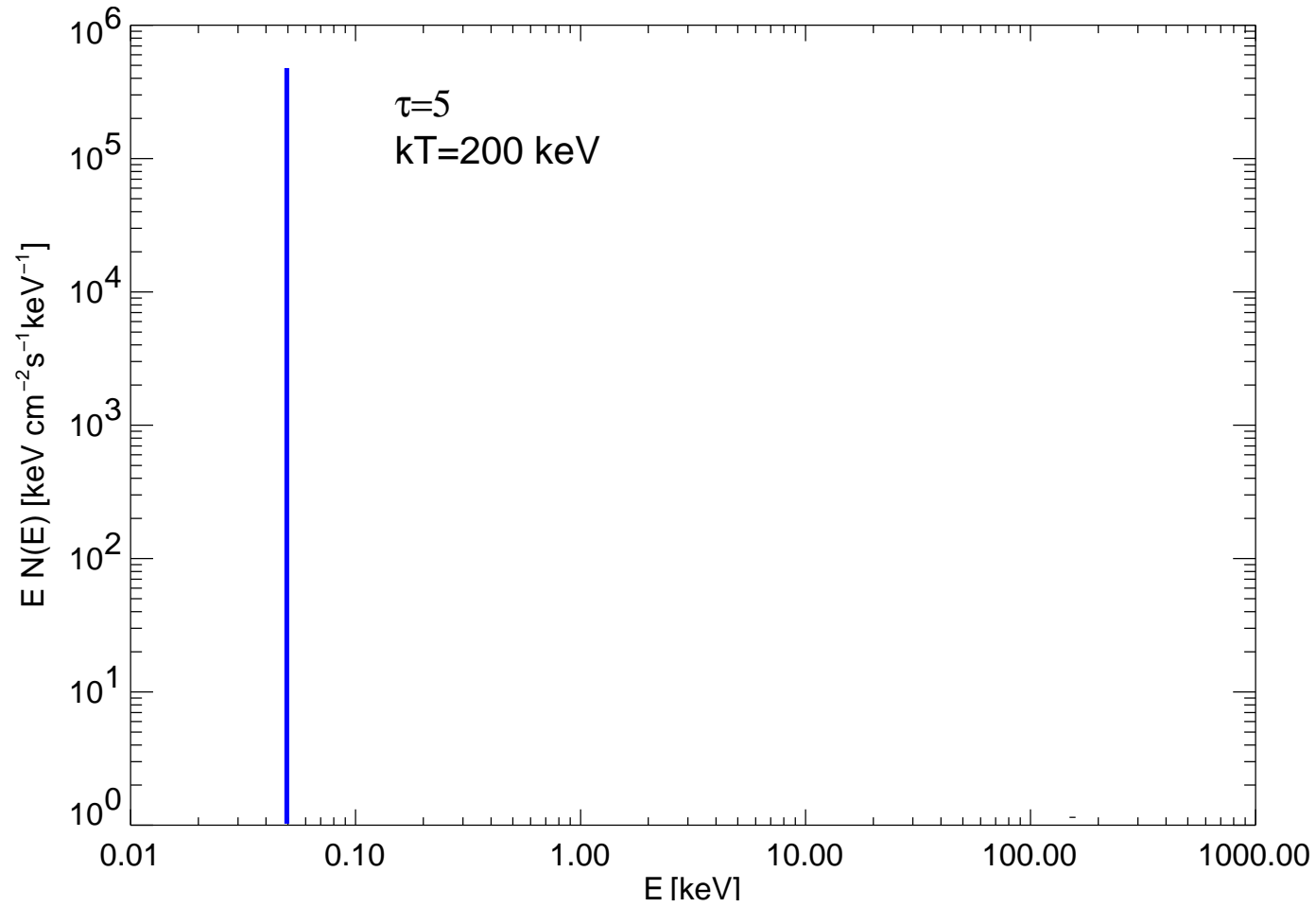
Comptonization produces power-law spectra.

General solution: Possible via the [Monte Carlo method](#).



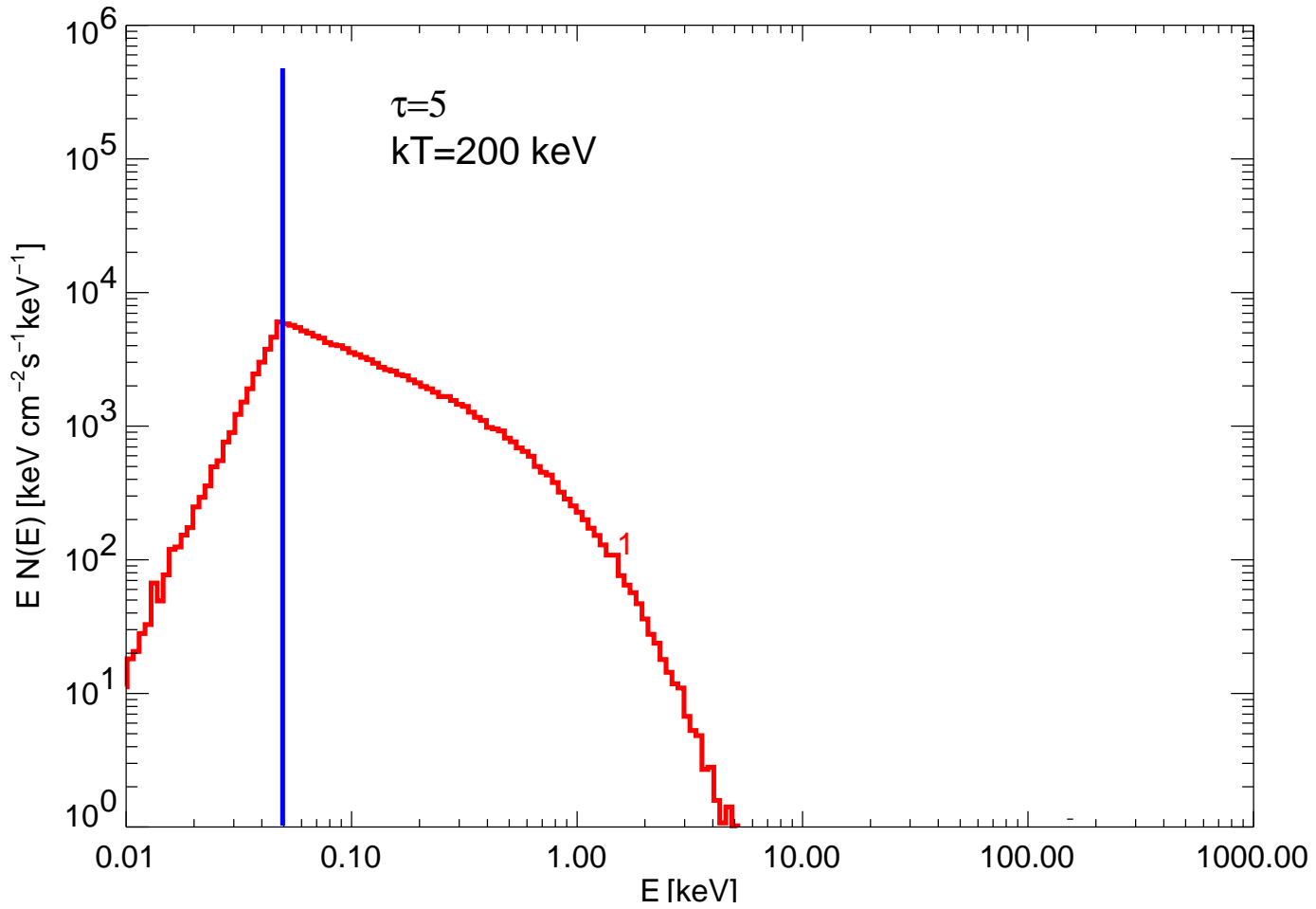


Spectral shape, III



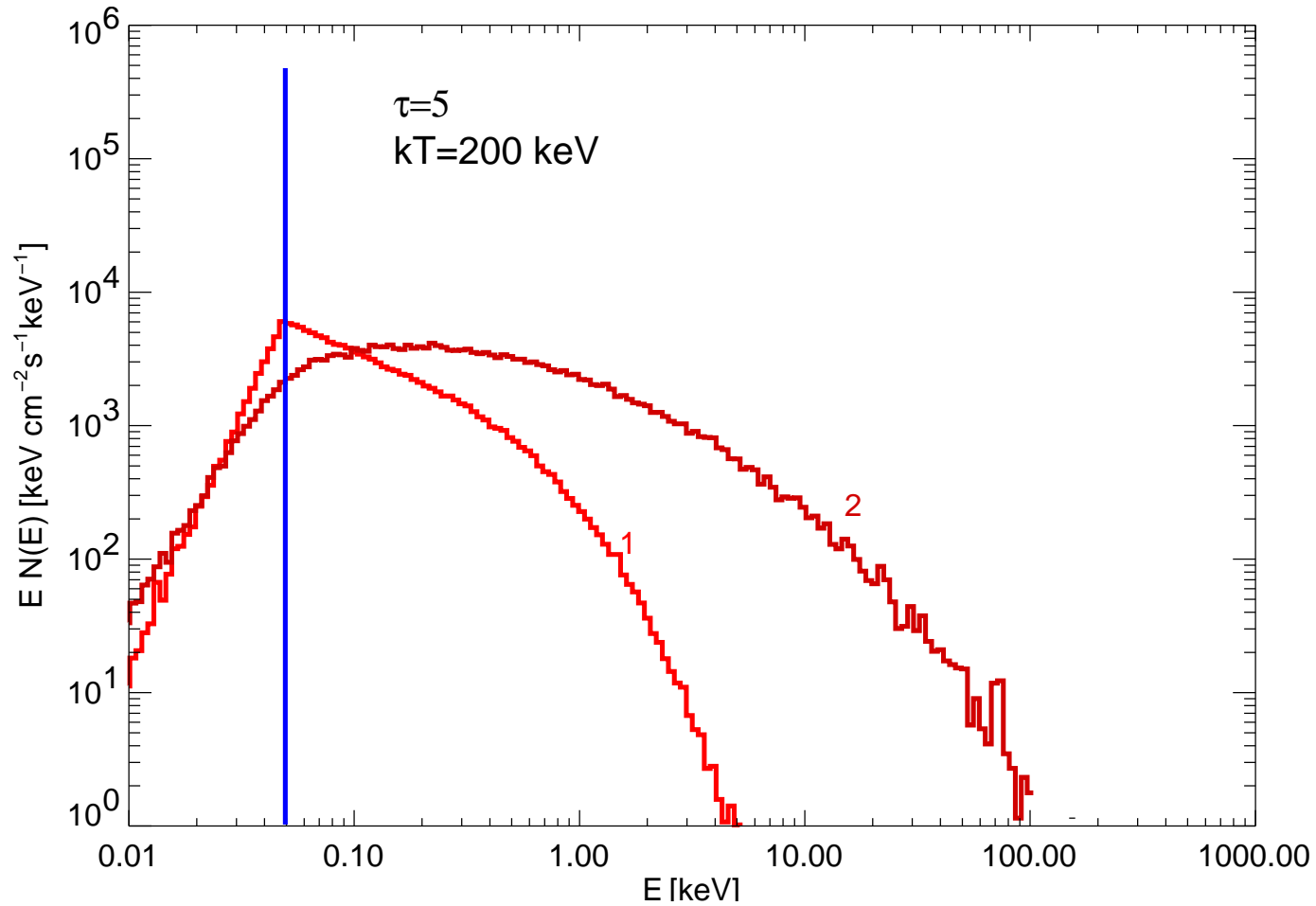


Spectral shape, IV



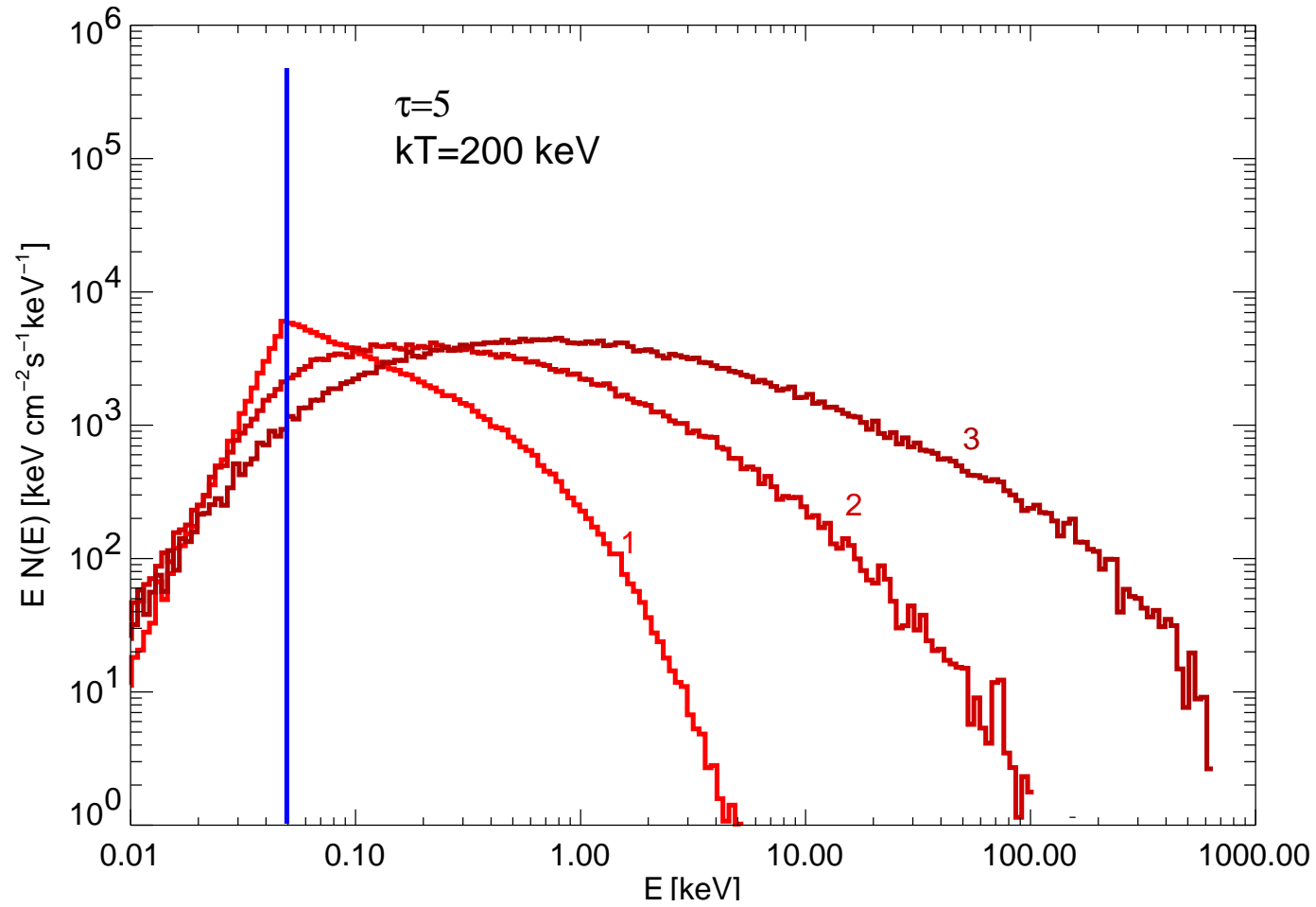


Spectral shape, V



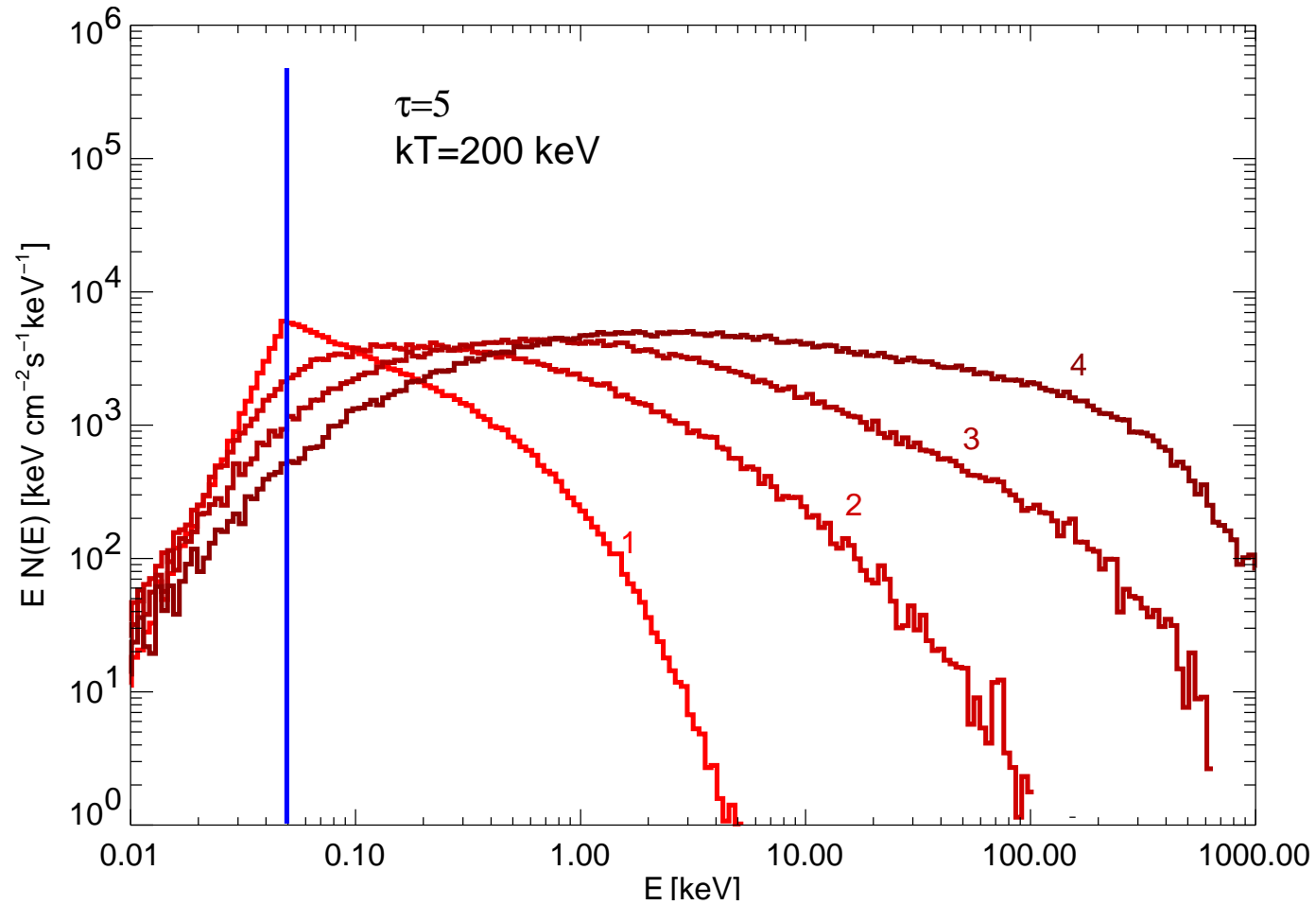


Spectral shape, VI



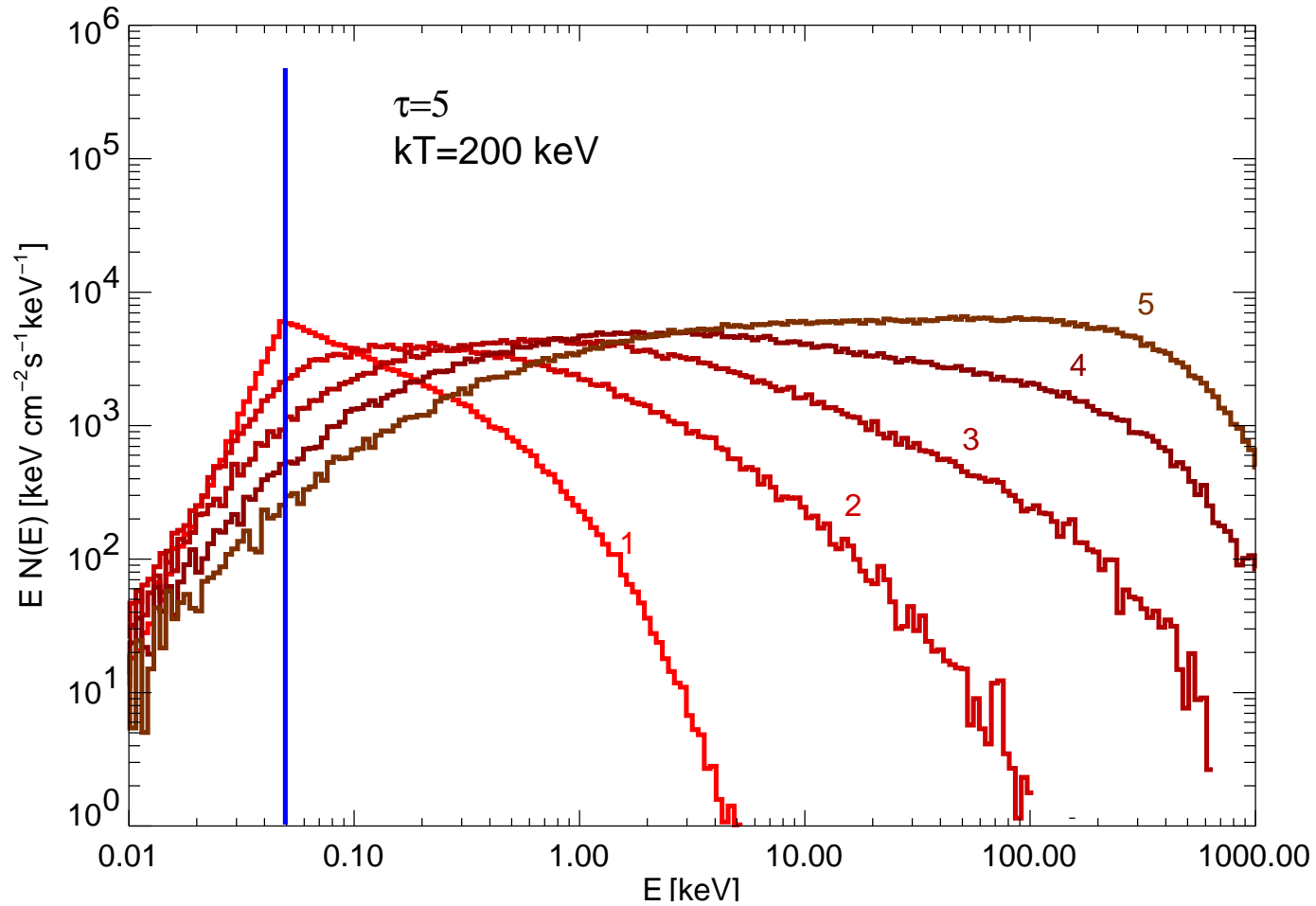


Spectral shape, VII



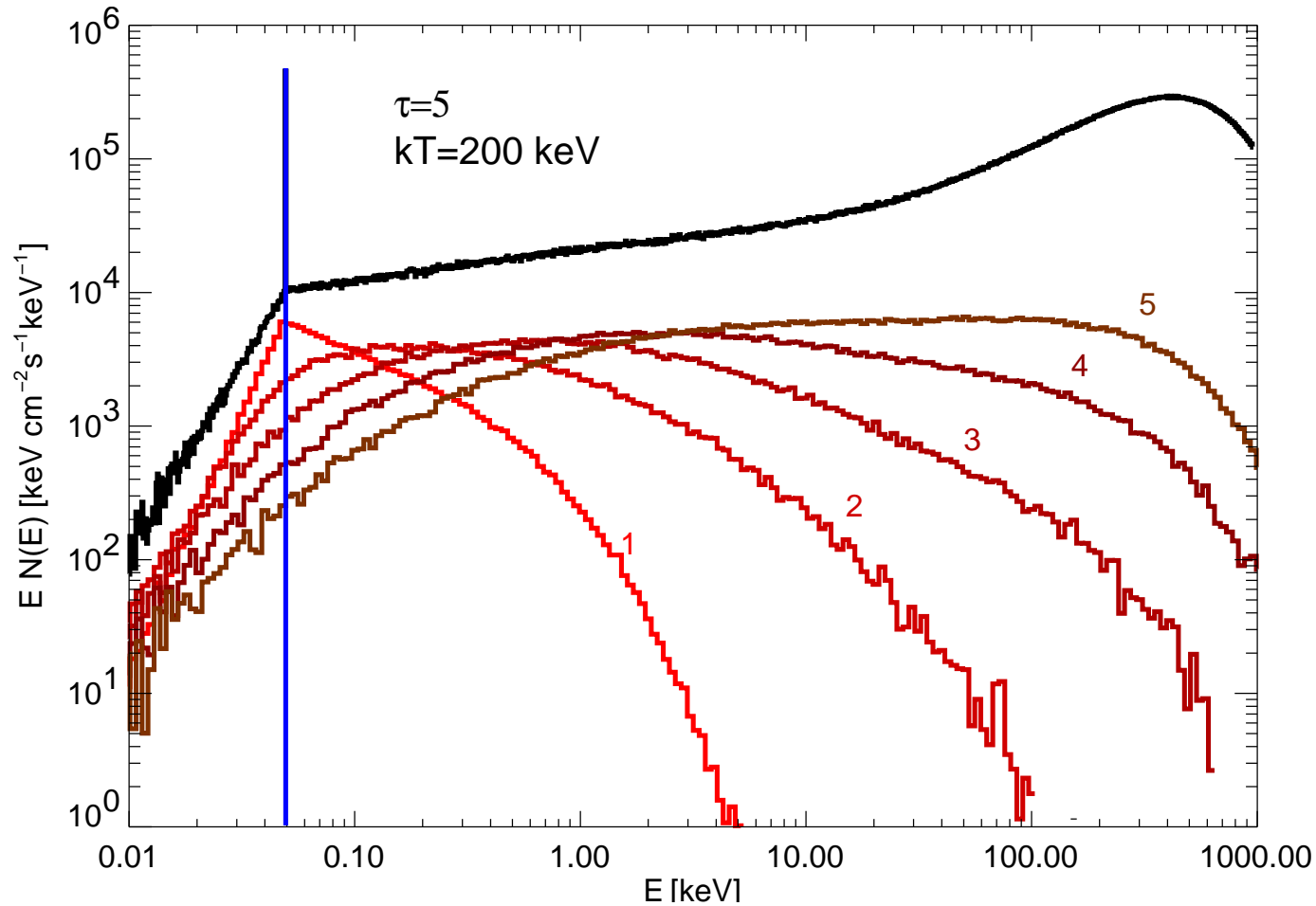


Spectral shape, VIII





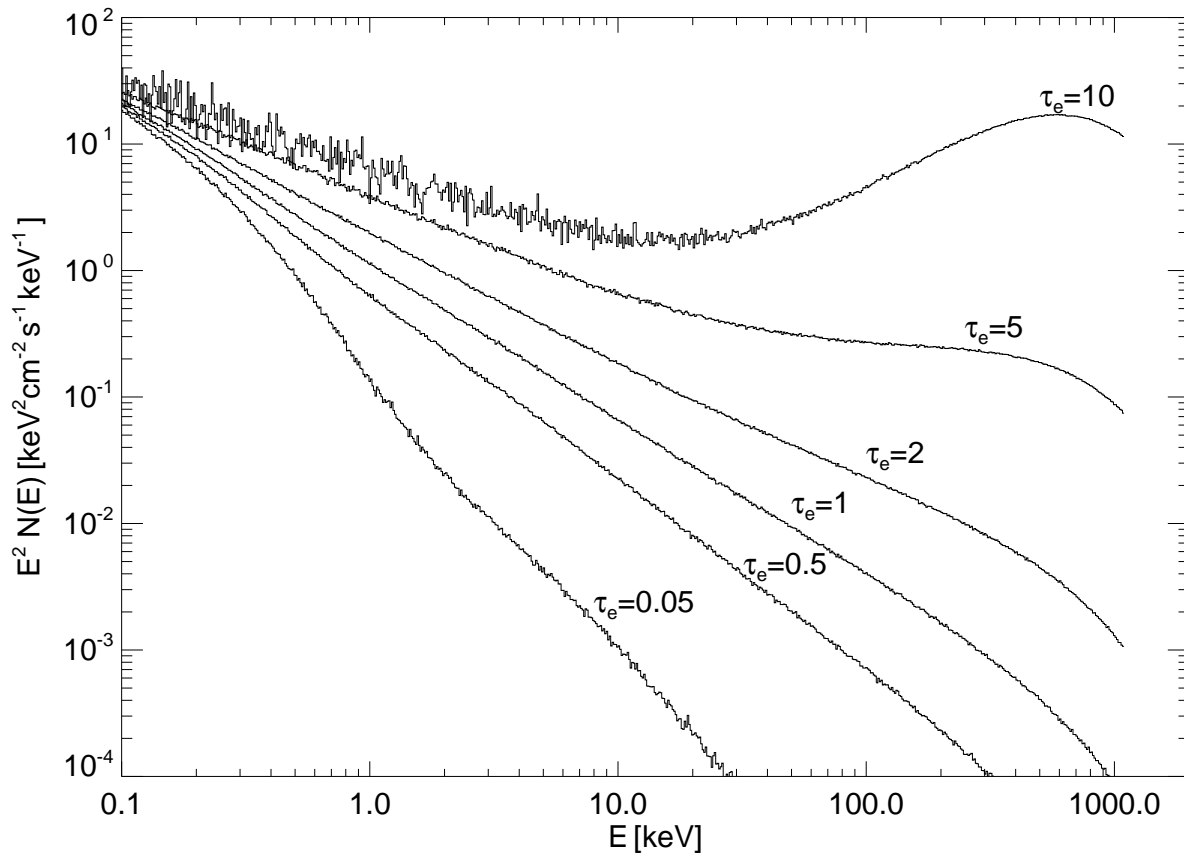
Spectral shape, IX



Monte Carlo simulation shows: Spectrum is \implies **Power law with exponential cutoff** (here: with additional “Wien hump”, see next slide)



Spectral shape, X



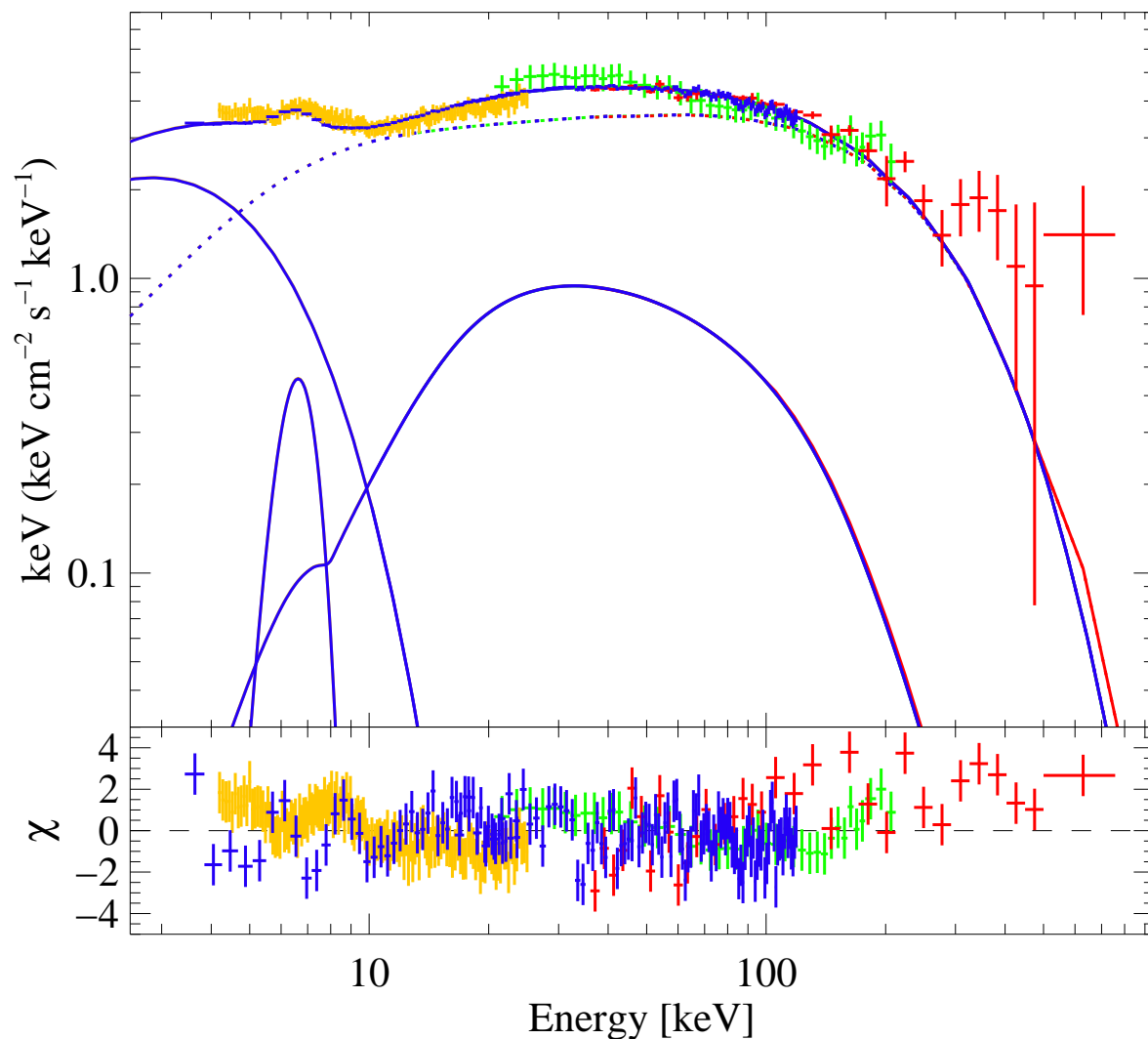
Sphere with $kT_e = 0.7m_e c^2$ (~ 360 keV), seed photons come from center of sphere.

$y \ll 1$: pure power-law.
 $y < 1$: power-law with exponential cut-off
 $y \gg 1$: “Saturated Comptonization”.

Saturated Comptonization has never been observed.



Galactic Black Holes



Fit of a *Comptonization* model to *RXTE/INTEGRAL* data from the galactic black hole Cygnus X-1.

$$kT_{\text{soft}} = 1.21 \text{ keV},$$

$$\tau_e = 1.09,$$

$$kT_e \sim 100 \text{ keV}$$

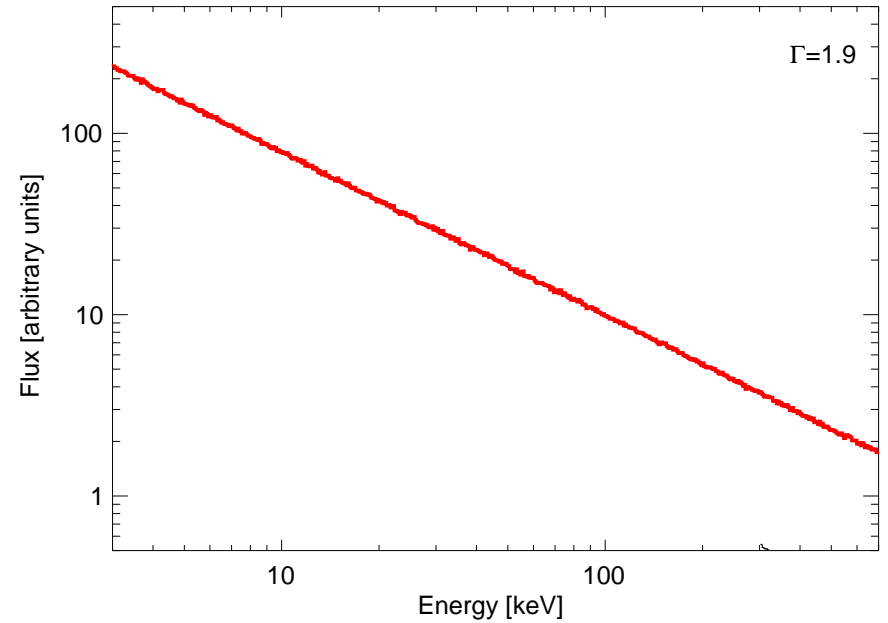
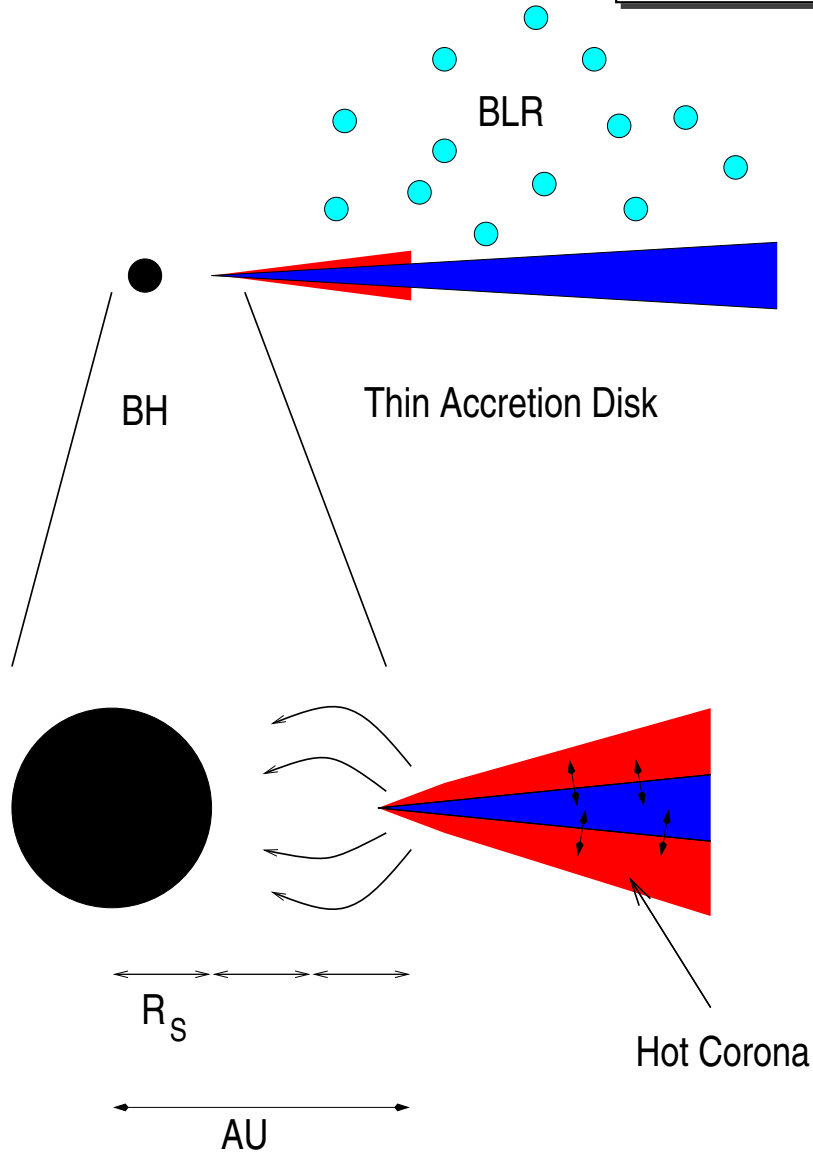
Model works extremely well \implies
Comptonization seems to explain
the data.

Note the presence of a **Compton reflection hump** (evidence of close vicinity of hot electrons and only mildly ionized material)

Fritz, et al., 2006



K α Line Diagnostics

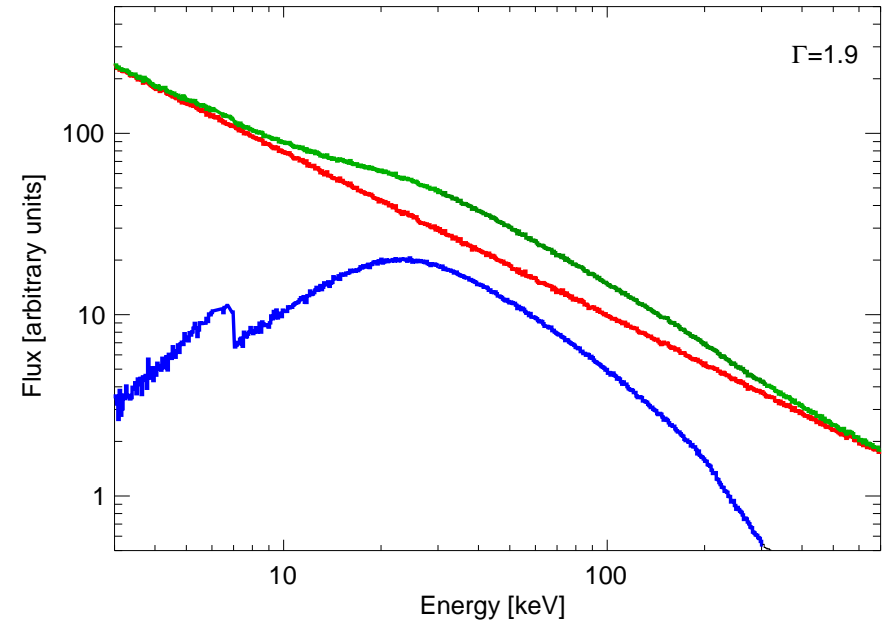
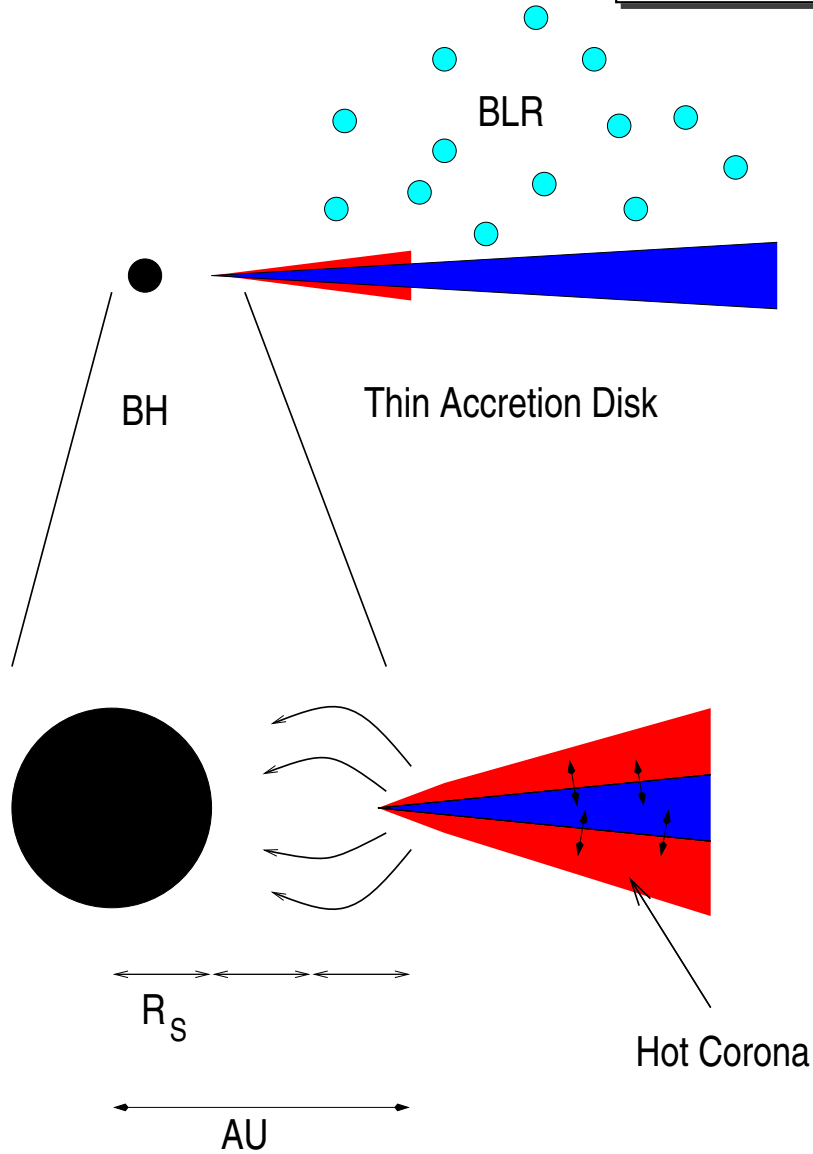


AGN X-Ray Spectrum:

- Comptonization of soft X-rays from accretion disk in hot corona ($T \sim 10^8$ K): power law continuum.



K α Line Diagnostics

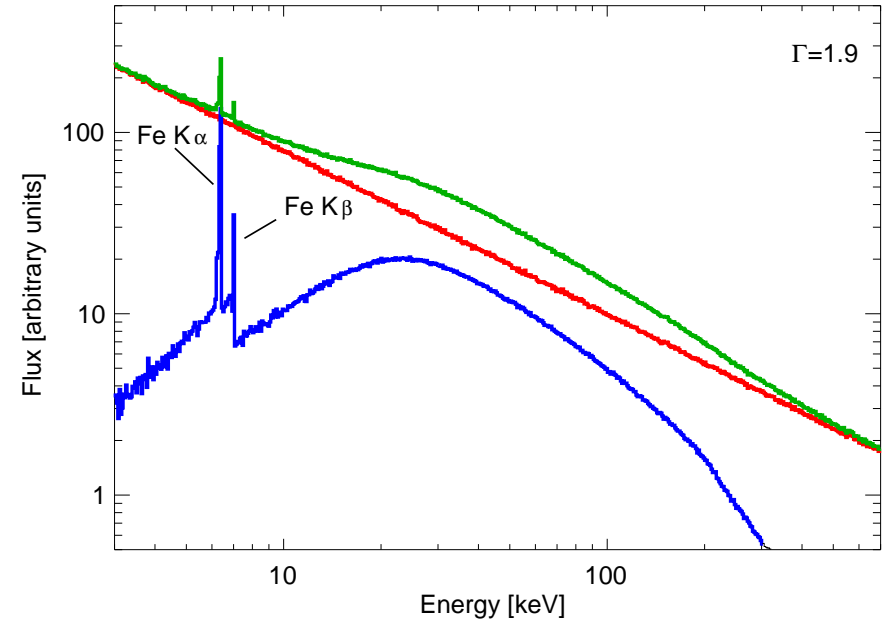
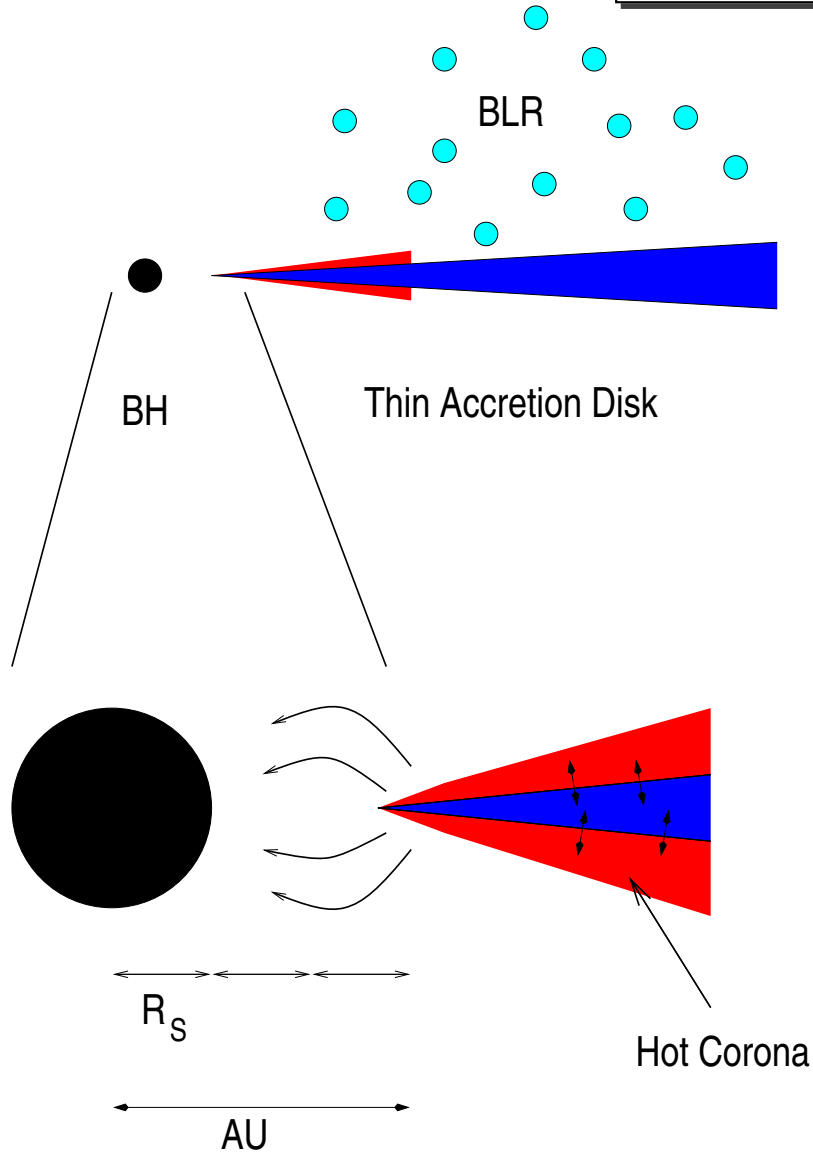


AGN X-Ray Spectrum:

- **Comptonization** of soft X-rays from accretion disk in **hot corona** ($T \sim 10^8$ K): **power law continuum**.
- **Thomson scattering** of power law photons in disk: **Compton Reflection Hump**



K α Line Diagnostics

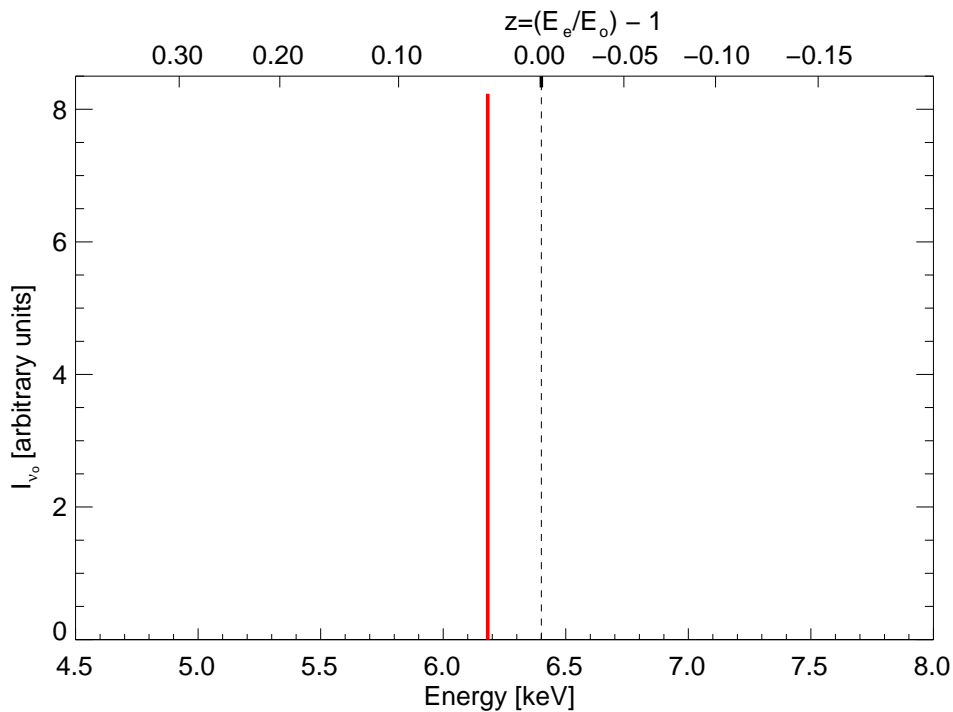
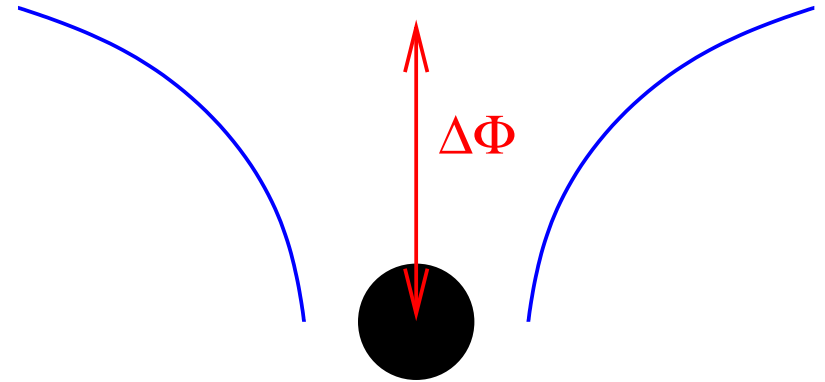


AGN X-Ray Spectrum:

- Comptonization of soft X-rays from accretion disk in hot corona ($T \sim 10^8$ K): power law continuum.
- Thomson scattering of power law photons in disk: Compton Reflection Hump
- Photoabsorption of power law photons in disk: fluorescent Fe K α Line at ~ 6.4 keV



K α Line Diagnostics

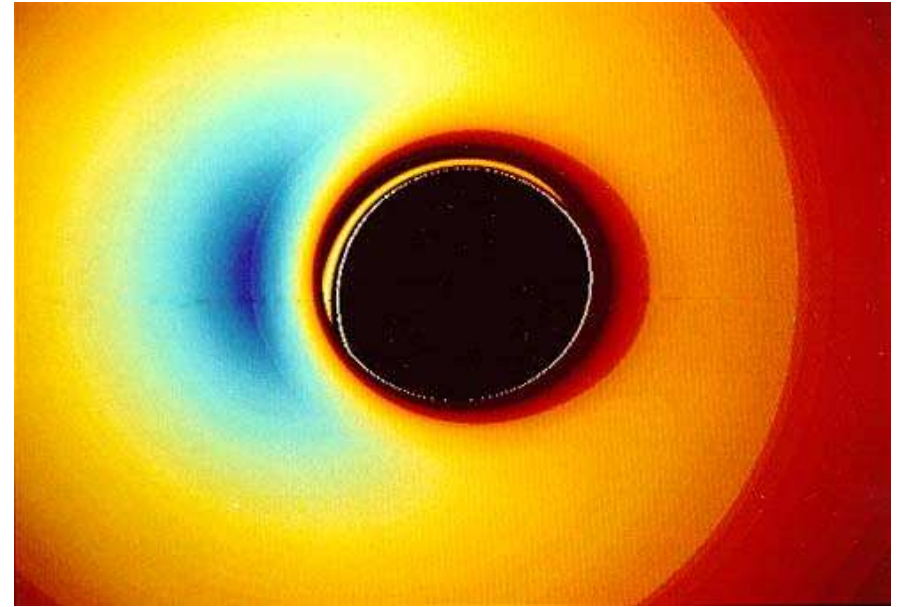
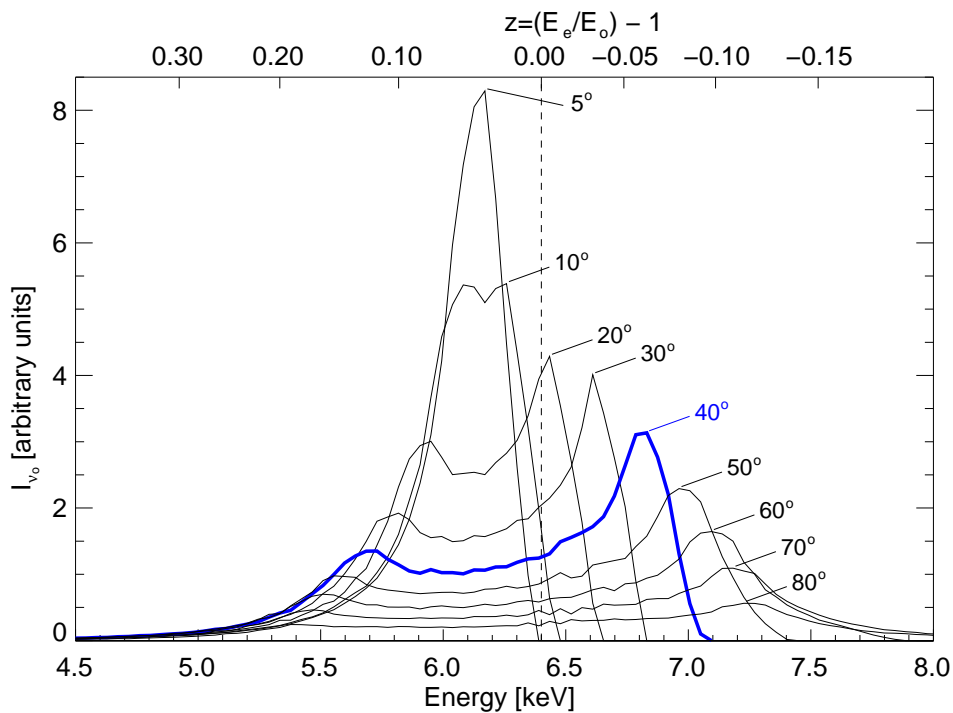
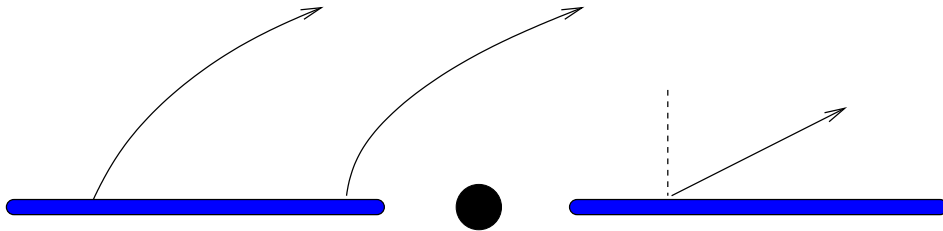


Total observed line profile affected by

- grav. Redshift



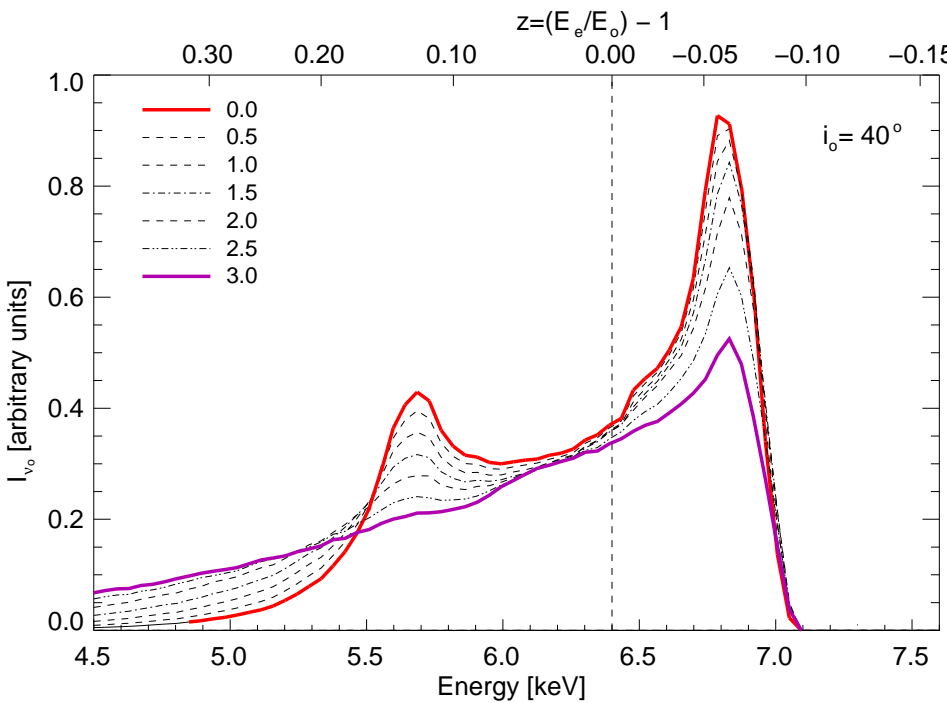
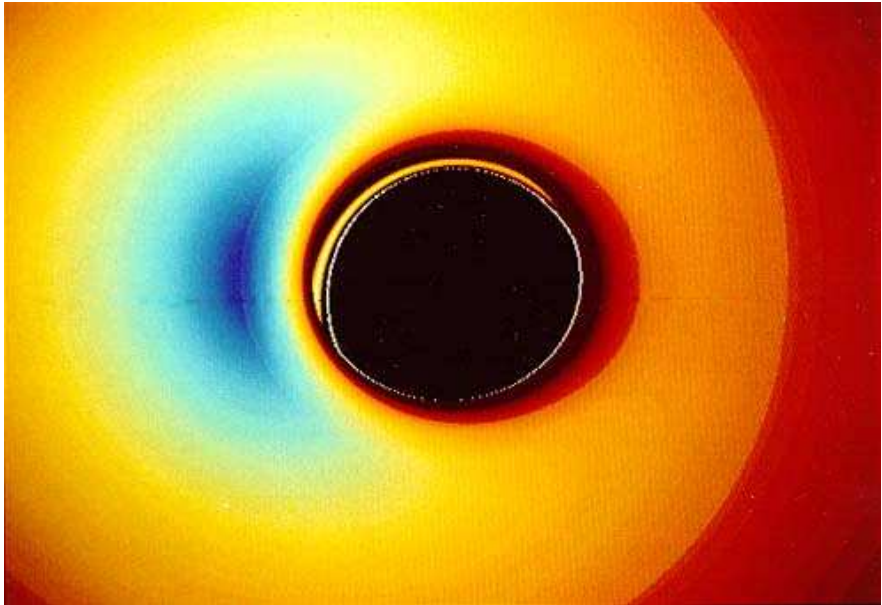
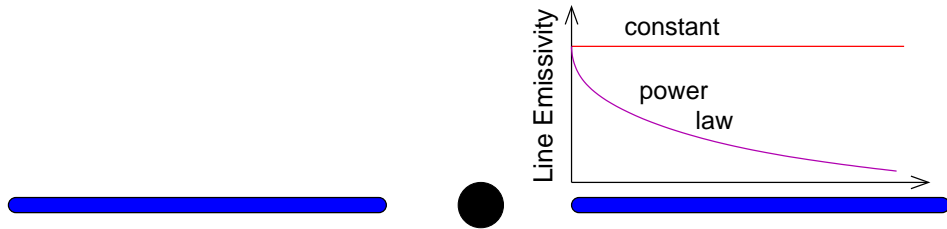
K α Line Diagnostics



Total observed line profile affected by

- grav. Redshift
- Light bending
- rel. Doppler shift

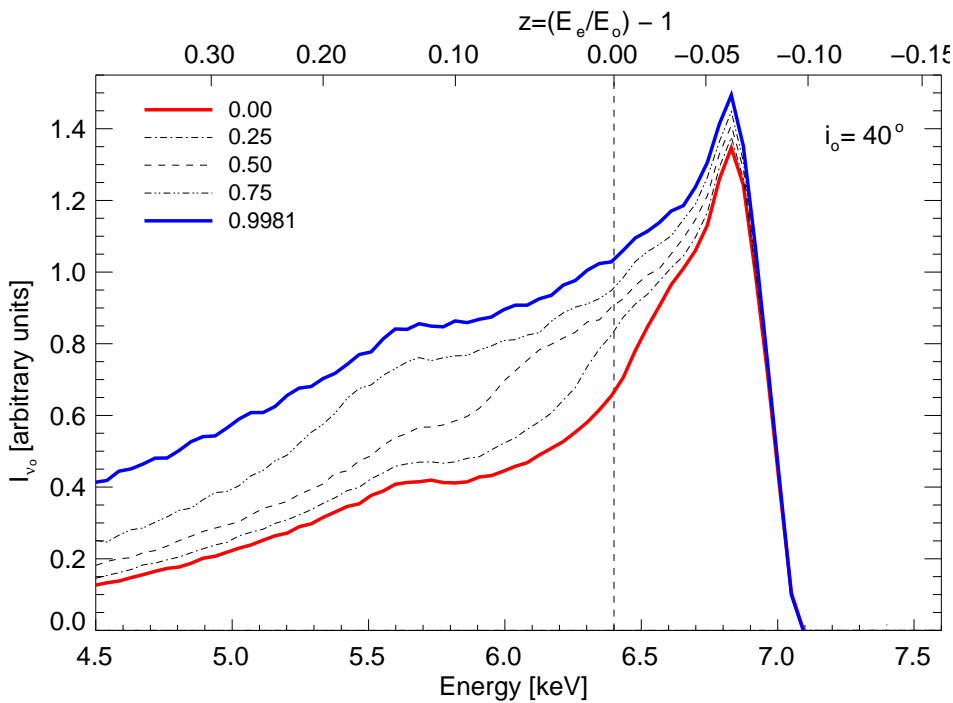
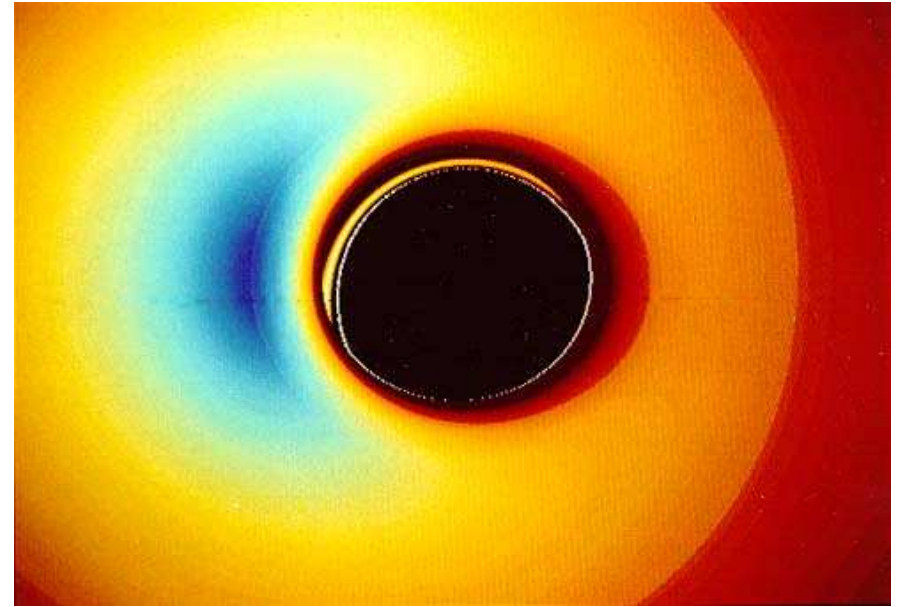
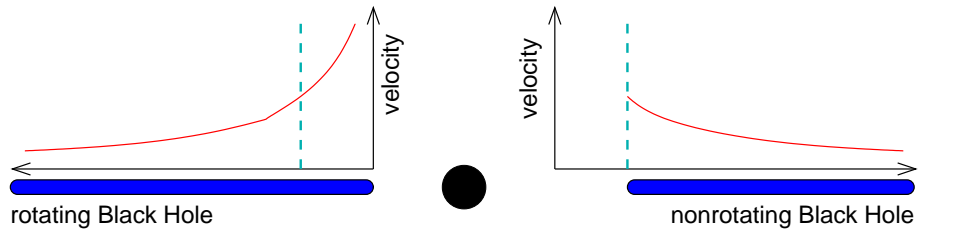
K α Line Diagnostics



Total observed line profile affected by

- grav. Redshift
- Light bending
- rel. Doppler shift
- emissivity profile

K α Line Diagnostics

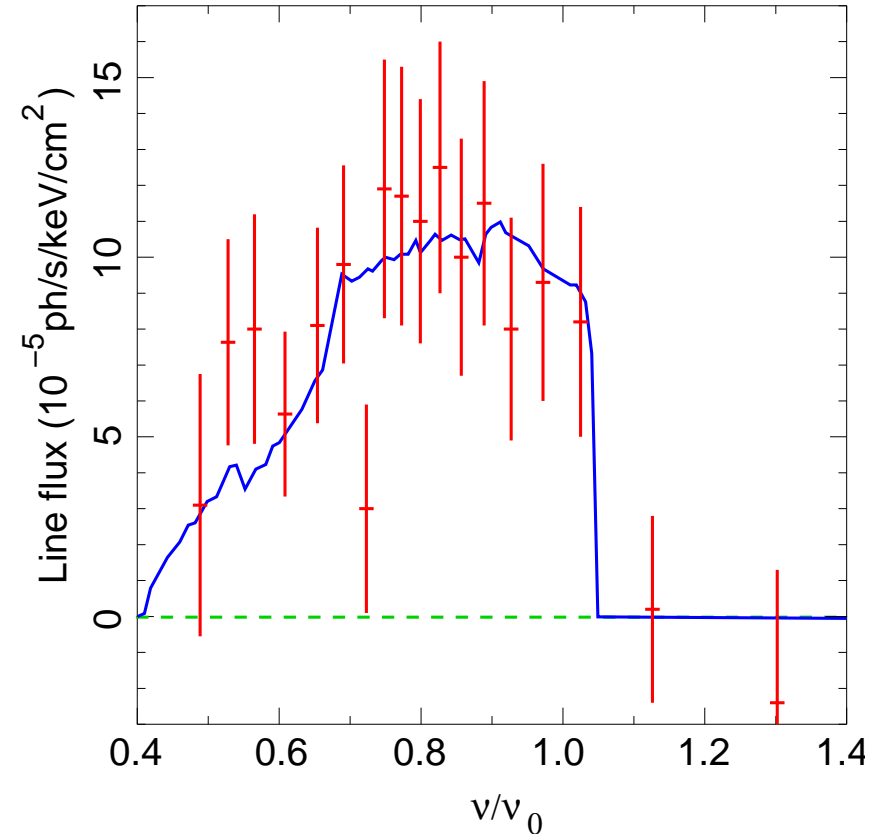
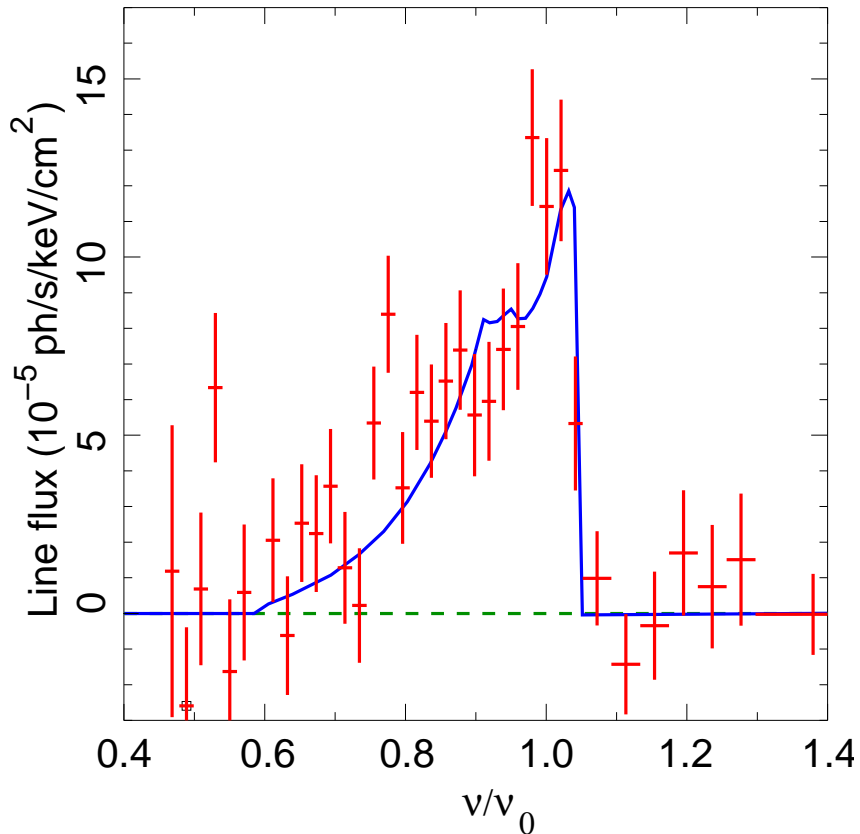


Total observed line profile affected by

- grav. Redshift
- Light bending
- rel. Doppler shift
- emissivity profile
- spin of black hole



MCG-6-30-15



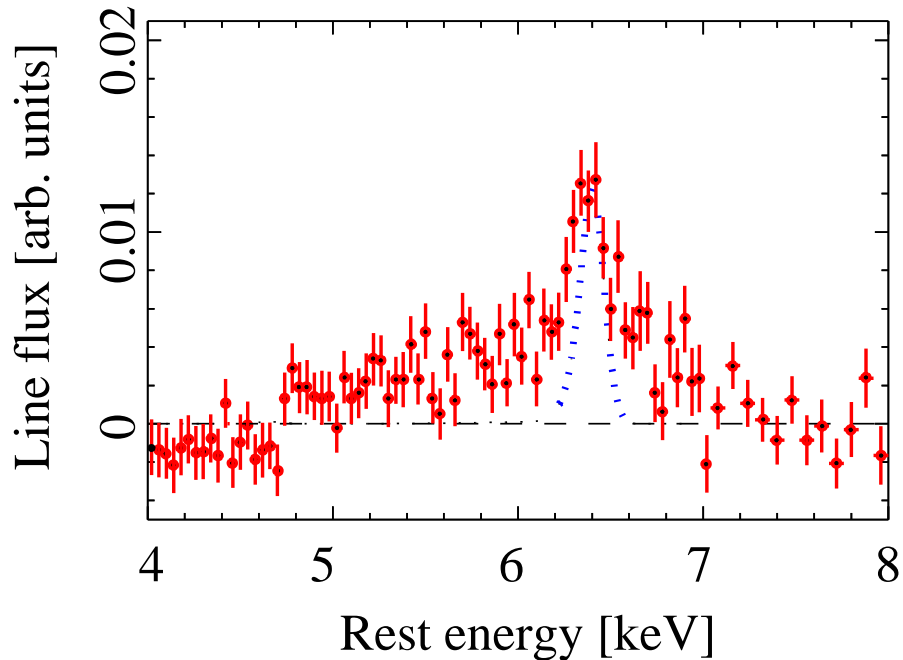
MCG-6-30-15 ($z = 0.008$): first AGN with relativistic disk line

Tanaka et al. (1995): time averaged *ASCA*
spectrum: line skew symmetric
 \Rightarrow Schwarzschild black hole.

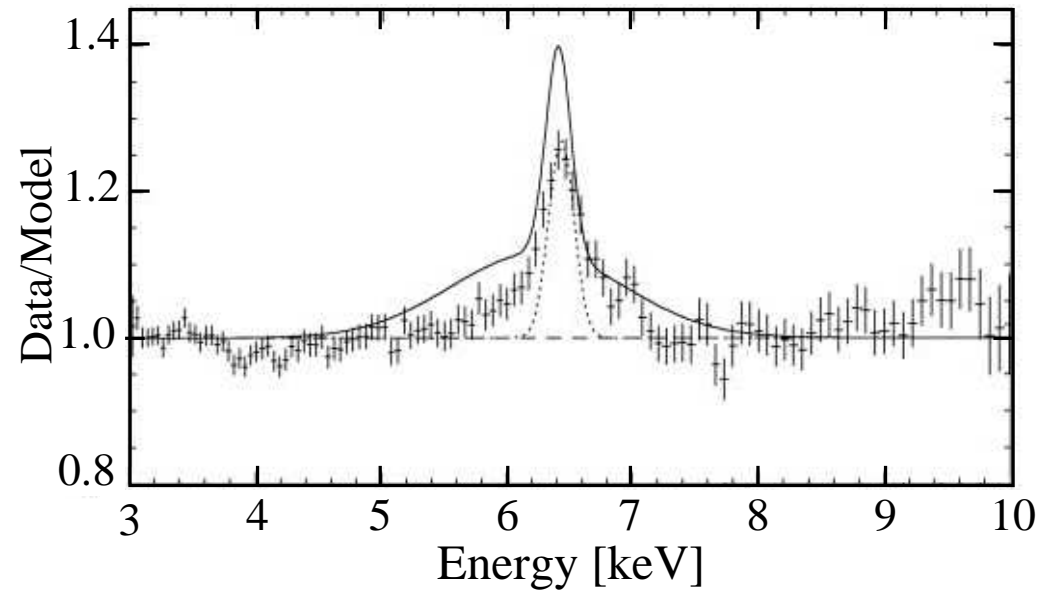
Iwasawa et al. (1996): “deep minimum
state”: extremely broad line
 \Rightarrow Kerr Black Hole.

Later confirmed with *BeppoSAX* (Guainazzi et al., 1999) and *RXTE* (Lee et al., 1999).

Broad Lines with ASCA



(Nandra et al., 1997, Fig. 4b)



(Lubiński & Zdziarski, 2001, Fig. 2a)

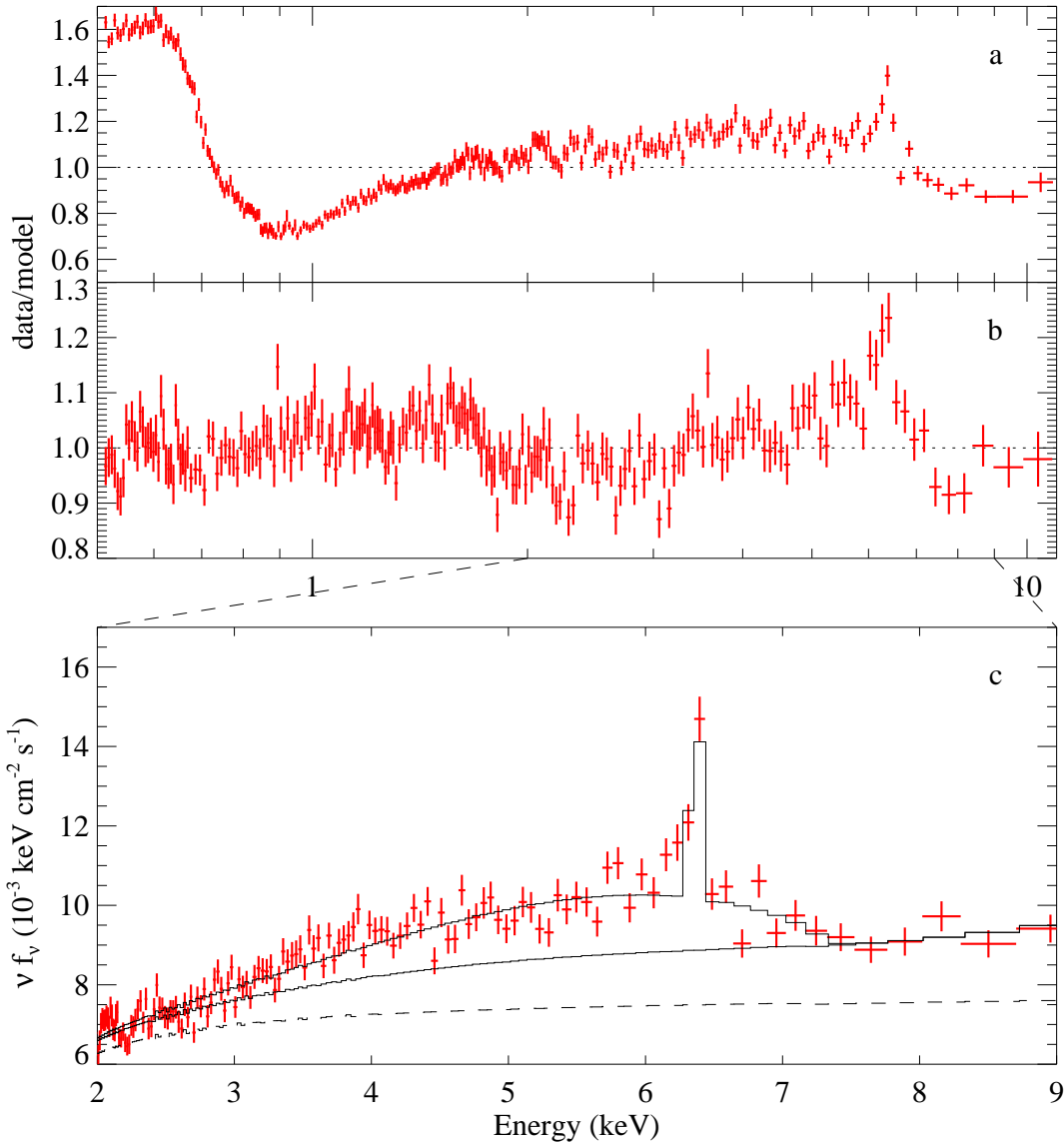
ASCA: Average Seyfert Fe $K\alpha$ profile contains a narrow core and a red and blue wings, but they are much weaker than MCG-6-30-15.

Best case: MCG-6-30-15





MCG-6-30-15, II



pure PL fit

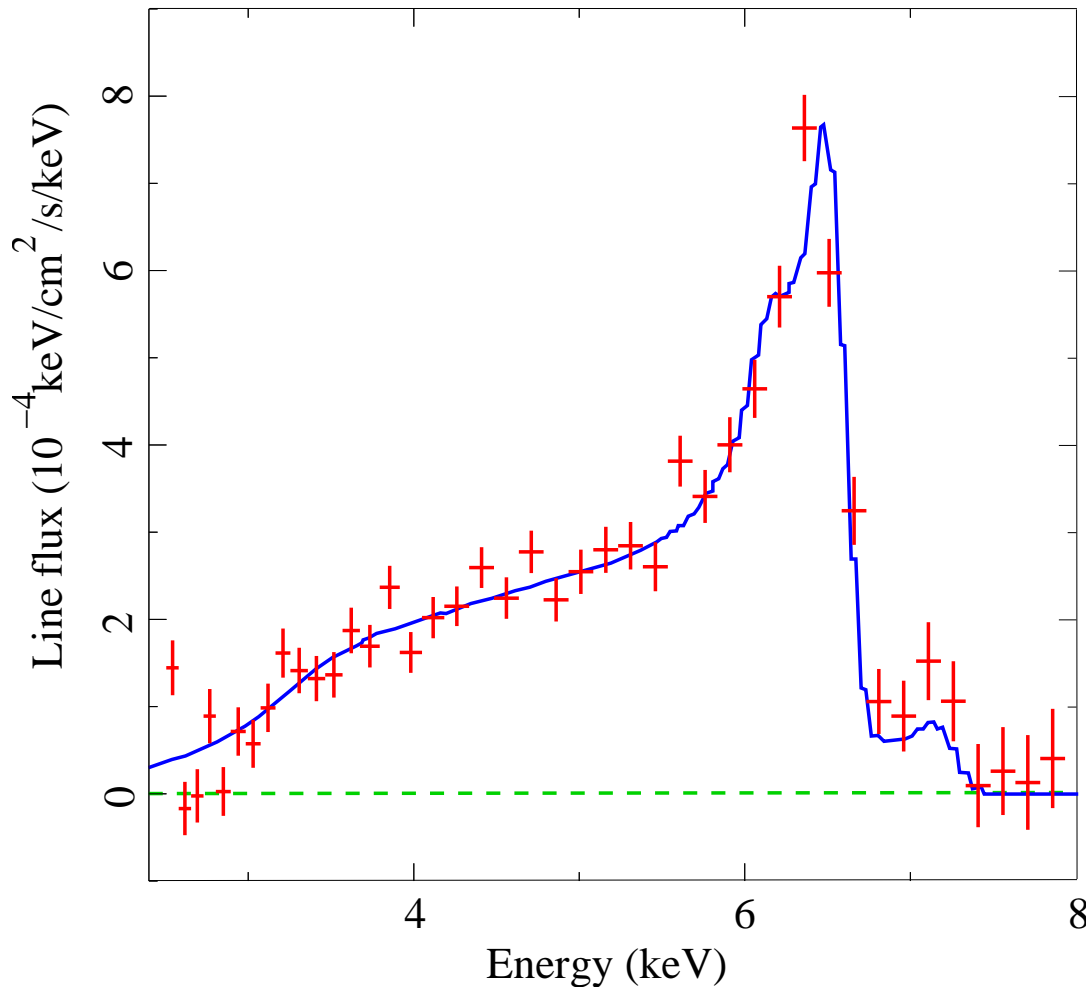
Better modeling of soft excess and reflection \implies Fe K α line has **extreme width and skewed profile**.

Components of the final fit
 \implies Line emissivity is strongly concentrated towards the inner edge of the disk ($\epsilon \propto r^{-4.6}$; cannot be explained with standard α -disk)

(XMM-Newton, June 2000, 100 ksec; Wilms et al., 2001)



MCG-6-30-15, III



Fabian et al. (2002)

2001 July/August: 315 ksec
observation

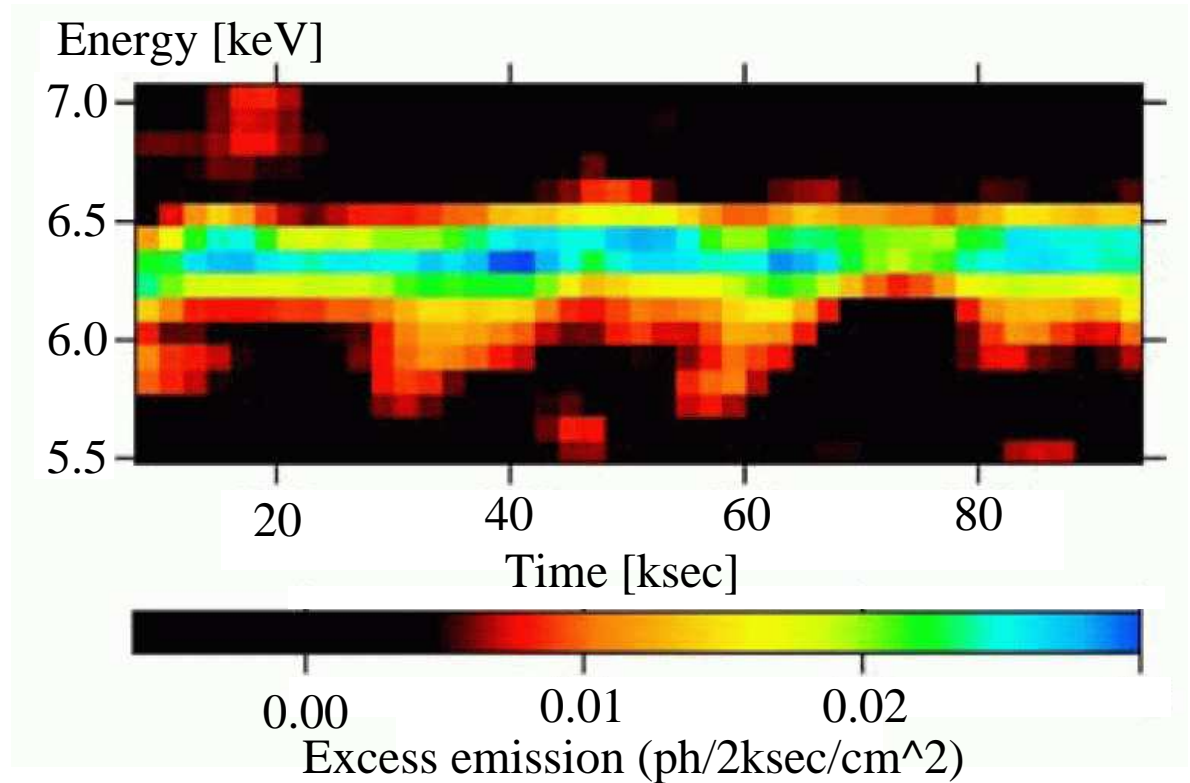
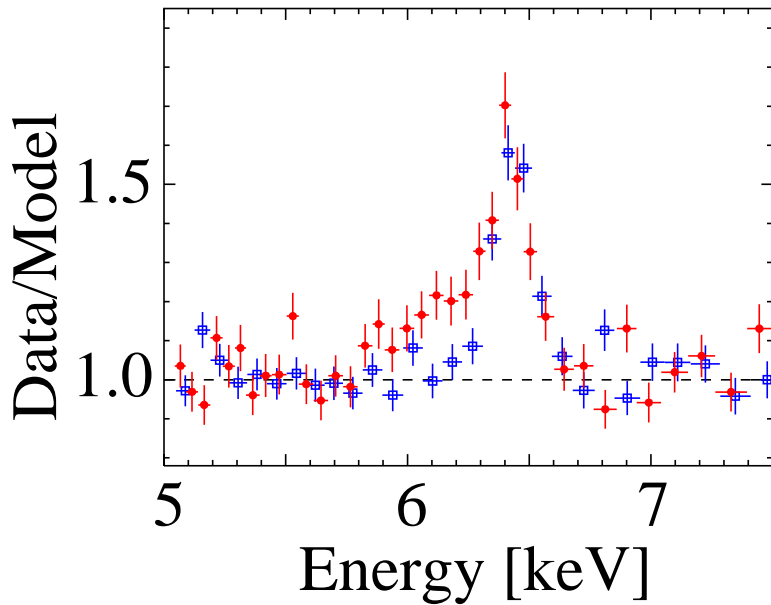
(Fabian et al., 2002)

- Strong narrow line
- broad line clearly present
- **emissivity profile very steep for radii close to r_{in}**

$$I_{\text{Fe K}\alpha} \propto r^{-5.5 \pm 0.3} \text{ for } r < 6.1^{+0.8}_{-0.5} r_g,$$
$$\propto r^{-2.7 \pm 0.1} \text{ outside that;}$$

Fabian & Vaughan (2003); confi rms
Wilms et al. (2001)

Other Sources



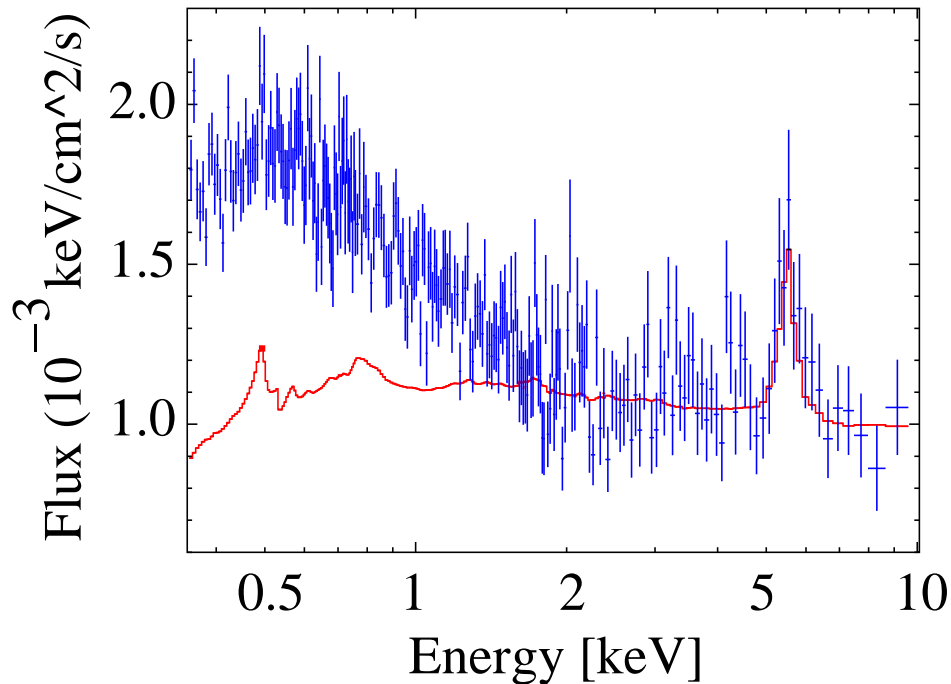
(Iwasawa, Miniutti & Fabian, 2004, Figs. 3,4)

Line profile variability in **NGC 3516** \implies **Corotating flare?** ($7r_g \lesssim r \lesssim 16r_g$)

If interpretation is pushed further, gives $M \sim (1 \dots 5) \times 10^7 M_\odot$.

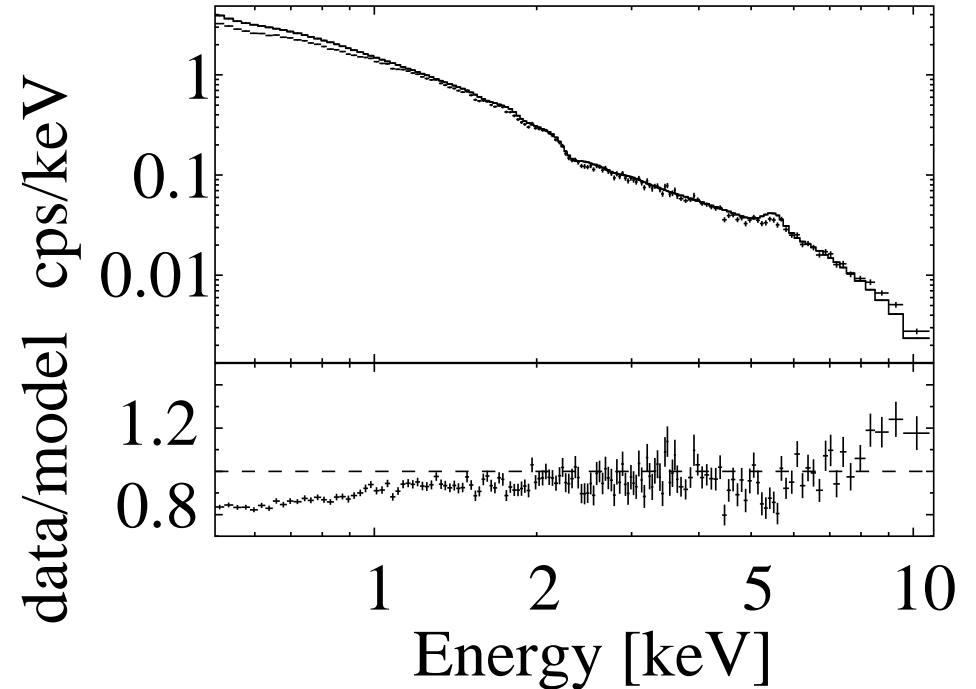


Other Sources



(Porquet & Reeves, 2003, Fig. 3)

XMM data from 2001



(Matt et al., 2005, Fig. 1)

comparison 2003 vs. 2001 data

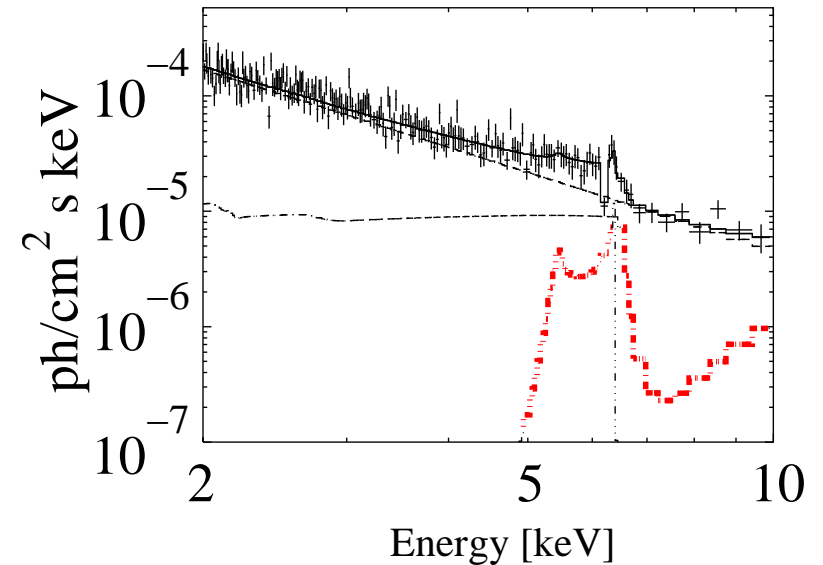
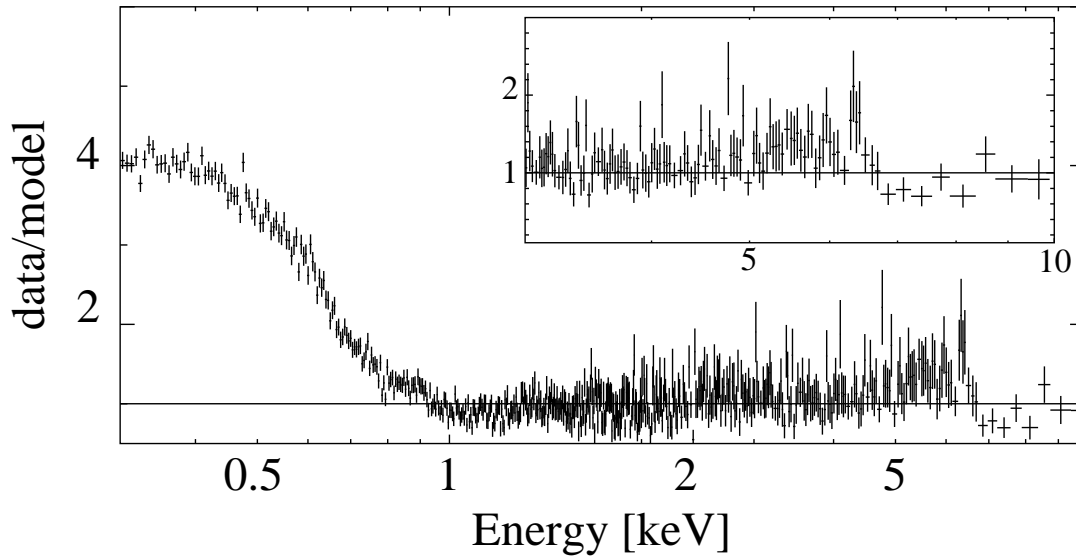
Q0056-363 (broad line radio-quiet quasar, $L_X > 10^{45}$ erg s⁻¹):

Fe K α has FWHM **24500 km s⁻¹**, EW 275 eV

Q0056-363 is highest luminosity radio-quiet QSO with broad Fe K α line.



Other Sources



(Longinotti et al., 2003)

IRAS 13349+2436:

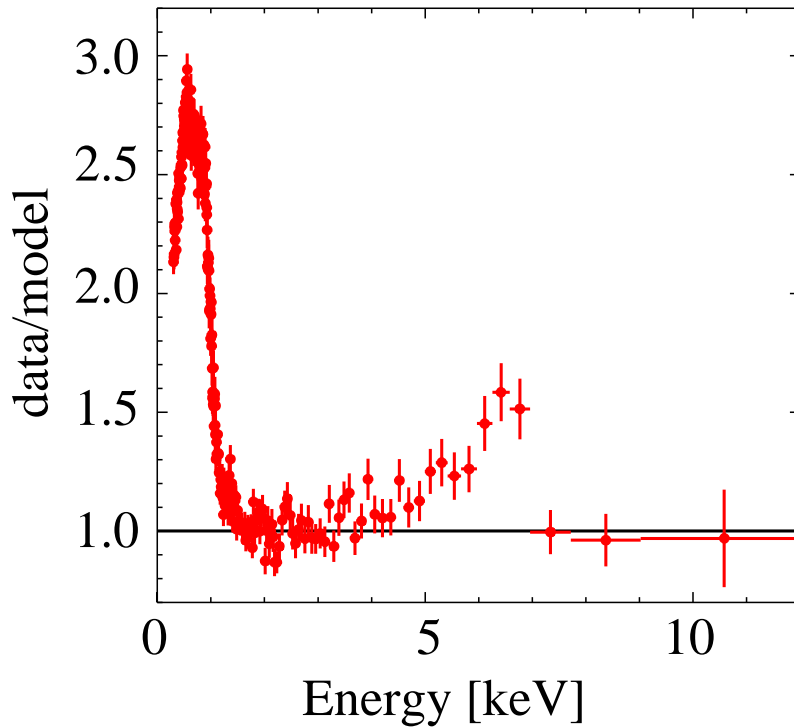
- Model either 2 broad emission lines *or*
- relativistic line from Fe XXIII/XXIV plus narrow absorption feature

Line shape can be rather complex!

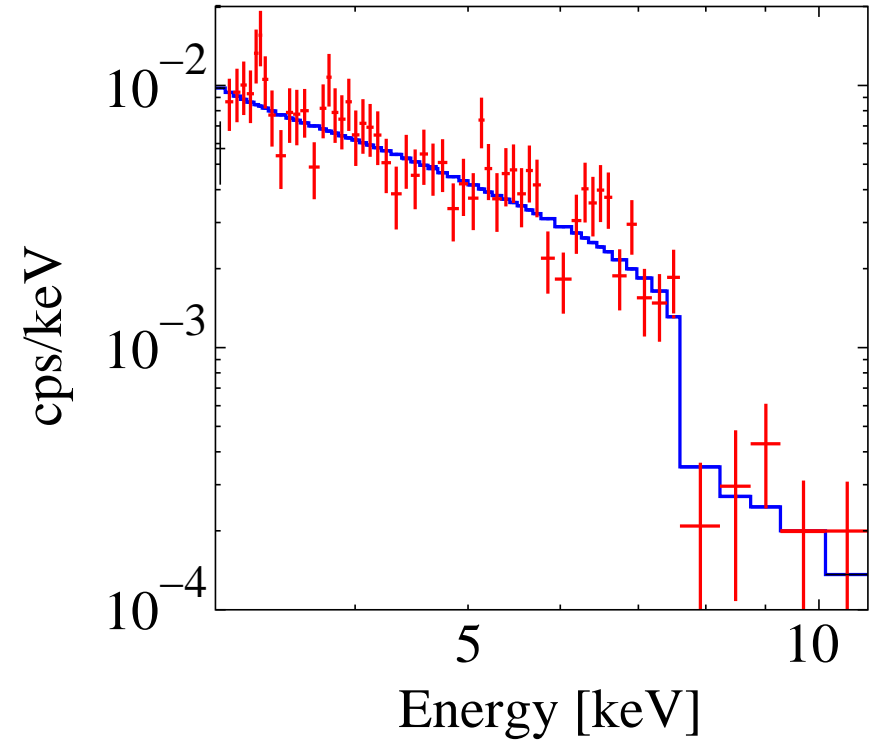
Other examples include *blueshifted* lines, e.g., in Mkn 205 (Reeves et al., 2001) or Mkn 766.



Absorption or Lines?



(1H0707-495; Fabian et al., 2004)



(IRAS 13224-3809; Boller et al., 2003)

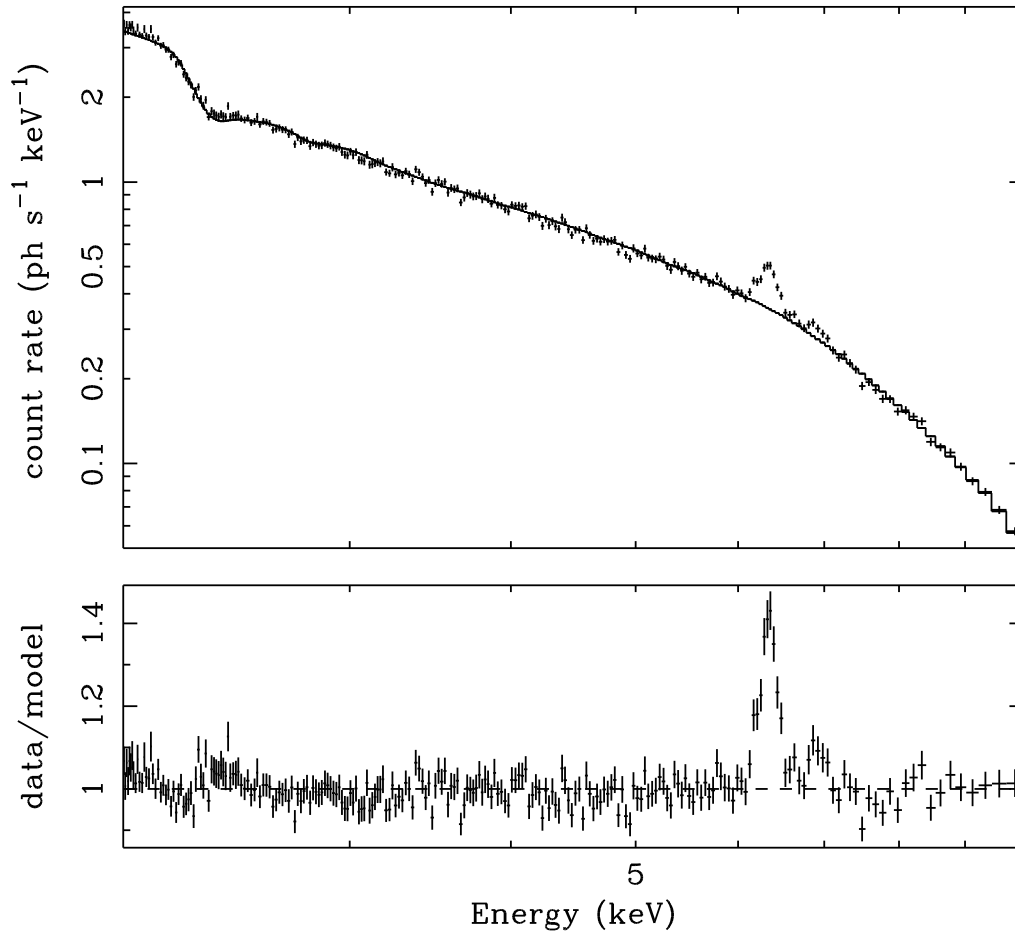
NLSy1: Strong absorption or a relativistic line from a reflection dominated spectrum both describe the data equally well!

Similar results have been found by Pounds et al. in a variety of sources...

But: strong absorption models contradict observations where data > 10 keV available.



Narrow Lines

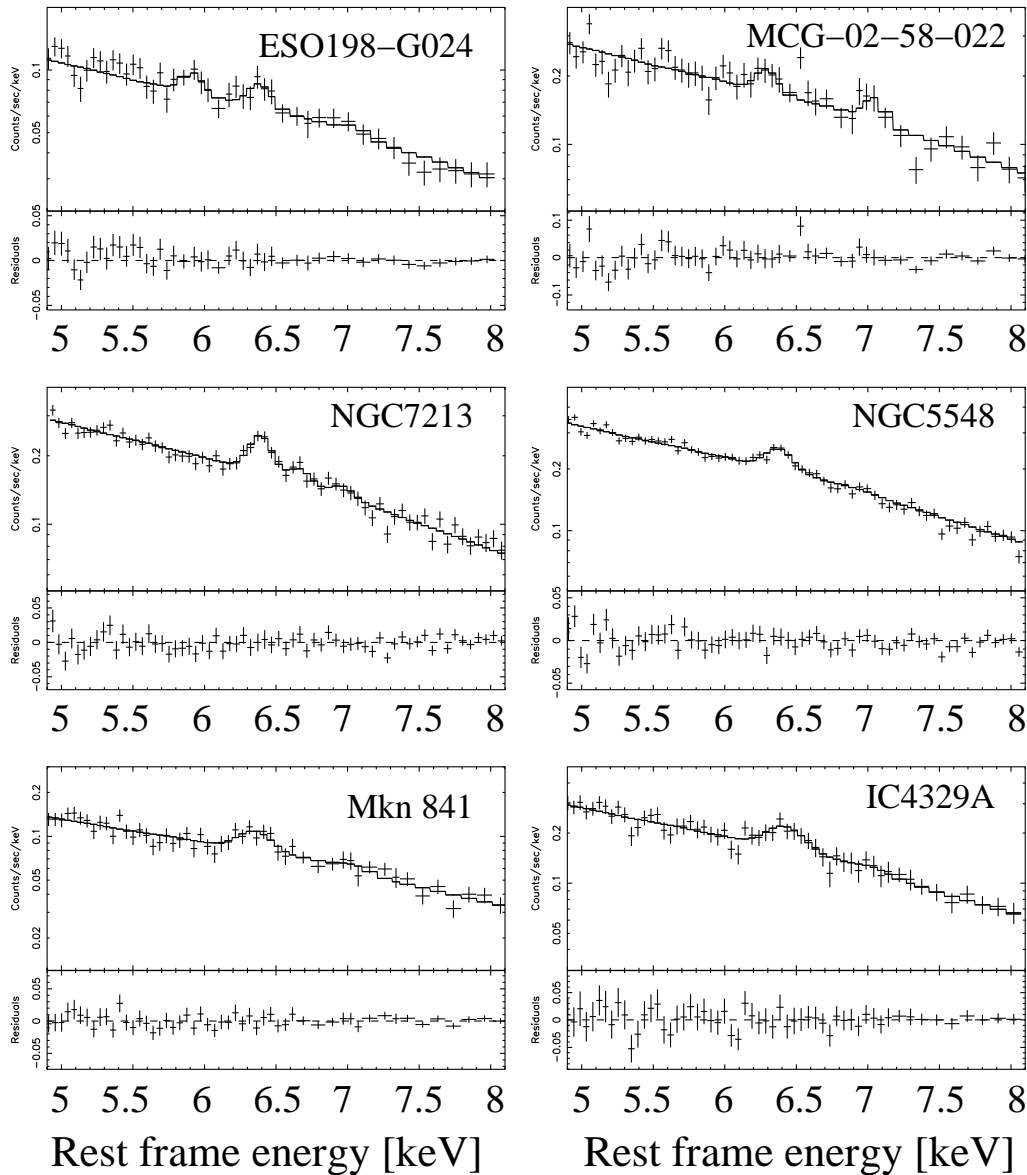


(NGC 4258; Reynolds et al. 2004)

The majority of Seyfert galaxies and QSOs do *not* show evidence for broad Fe $K\alpha$ lines!



Narrow Lines



The majority of Seyfert galaxies and QSOs do *not* show evidence for broad Fe $K\alpha$ lines!

statistics for PG-QSO: 20/38 show Fe $K\alpha$ line, of these 3 have broad line (Jiménez-Bailón et al., 2005)

Bianchi et al. (2004, Fig. 4)
[Sample of Seyferts with simultaneous *BeppoSAX* observations.]

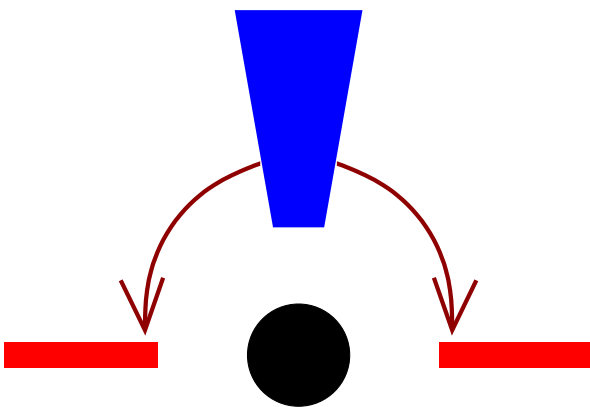
Conclusions, I

Relativistically broadened Fe $K\alpha$ lines clearly do exist in a variety of different AGN

We need to rethink the details of the accretion process and the accretion geometry close to black hole:

- Energy extraction for extremely broad lines?

Coupling BH – disk, structure of the inner disk (no torque condition?, structure of the infall region,...)



- “Lamppost model”?

(Petrucci & Henri, 1997; Martocchia, Matt & Karas, 2002; Miniutti & Fabian, 2004)

⇒ X-rays focused down from the jet base?

⇒ If true, is continuum Comptonization?

Fender et al. (2004), Markoff, Nowak & Wilms (2005) for galactic BHs



Conclusions, II

To be successful, models will have to consider:

- **Broad Fe $K\alpha$ lines are rare:**

- **Truncated Disks?**

- e.g., invoked by Zdziarski et al. (1999) to explain $\Omega/2\pi$ - Γ -correlation

- **Disk ionization** (but needs fine tuning!)

- **And what about the Unified Model?**

- Is the viewing angle really edge on?

- **Narrow lines are ubiquitous:**

- Are they formed in the **torus**?

- but narrow lines often have $\text{FWHM} \sim 4000\text{--}7000 \text{ km s}^{-1}$

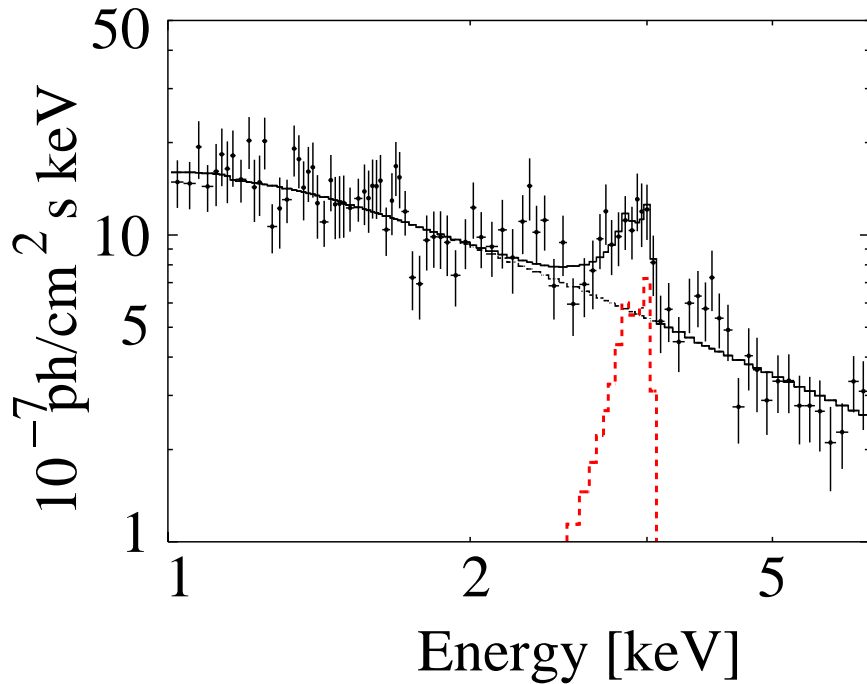
- \implies too large for torus! (expect $\sim 760 \text{ km s}^{-1} (M_8/r_{\text{pc}})^{1/2}$)

- Do they originate in the **BLR** or an **ionized disk**?

... and we should not forget the **observational constraints**: Strong Fe $K\alpha$ variability \implies **we need a larger collecting area (XEUS!)**



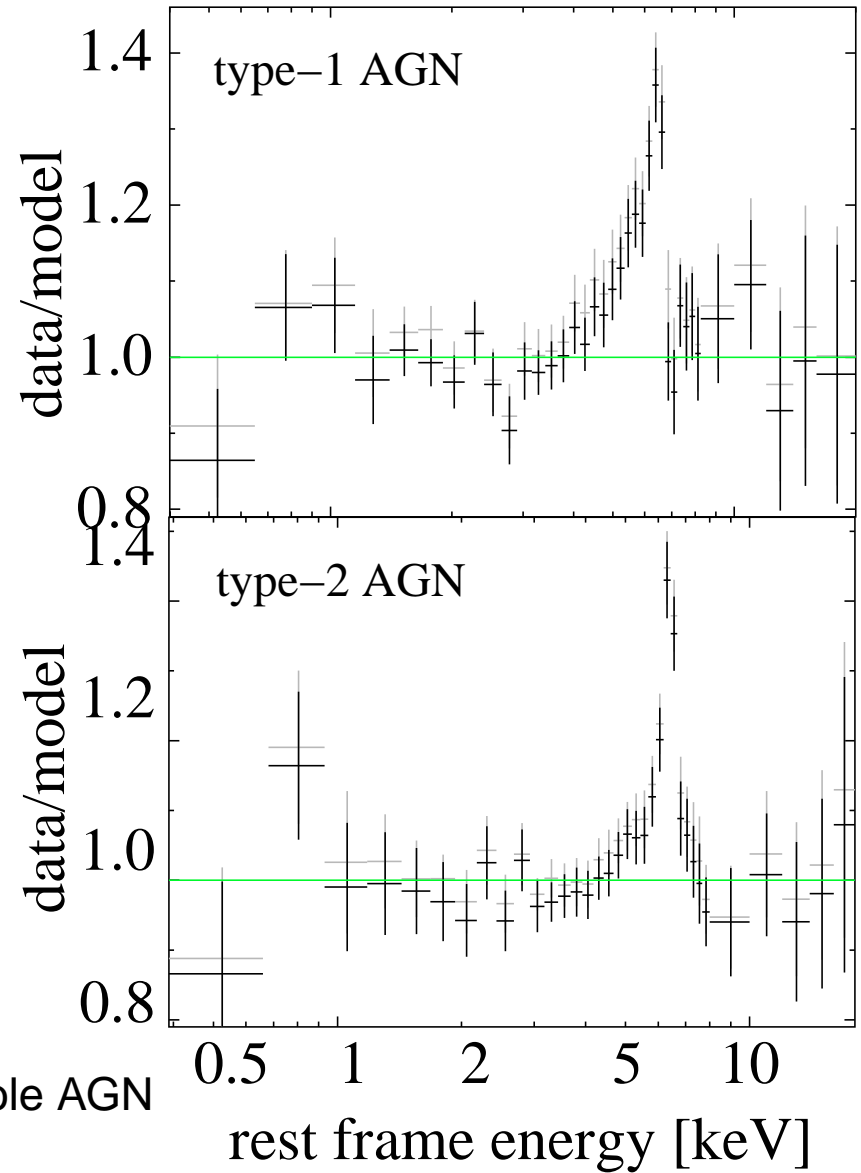
The Future



(Comastri, Brusa & Civano, 2004, *Chandra*)
CXO J123716.7+621733 (CDF-N; $z = 1.146$)

Broad Fe $K\alpha$ lines already present in high- z universe!

Average Fe line for the Lockman hole AGN
(Streblyanska et al., 2005)



- Bianchi, S., Matt, G., Balestra, I., Guainazzi, M., & Perola, G. C., 2004, *A&A*, 422, 65
- Boller, T., Tanaka, Y., Fabian, A., Brandt, W. N., Gallo, L., Anabuki, N., Haba, Y., & Vaughan, S., 2003, *MNRAS*, 343, L89
- Comastri, A., Brusa, M., & Civano, F., 2004, *MNRAS*, 351, L9
- Fabian, A. C., Miniutti, G., Gallo, L., Boller, T., Tanaka, Y., Vaughan, S., & Ross, R. R., 2004, *MNRAS*, 353, 1071
- Fabian, A. C., et al., 2002, *MNRAS*, 335, L1
- Guainazzi, M., et al., 1999, *A&A*, 341, L27
- Iwasawa, K., et al., 1996, *MNRAS*, 282, 1038
- Iwasawa, K., Miniutti, G., & Fabian, A. C., 2004, *MNRAS*, 355, 1073
- Jiménez-Bailón, E., Piconcelli, E., Guainazzi, M., Schartel, N., Rodríguez-Pascual, P. M., & Santos-Lleó, M., 2005, *A&A*, 435, 449
- Lee, J. C., Fabian, A. C., Brandt, W. N., Reynolds, C. S., & Iwasawa, K., 1999, *MNRAS*, 310, 973
- Longinotti, A. L., Cappi, M., Nandra, K., Dadina, M., & Pellegrini, S., 2003, *A&A*, 410, 471
- Lubiński, P., & Zdziarski, A. A., 2001, *MNRAS*, 323, L37
- Markoff, S., Nowak, M. A., & Wilms, J., 2005, *ApJ*, 635, 1203
- Martocchia, A., Matt, G., & Karas, V., 2002, *A&A*, 383, L23
- Matt, G., Porquet, D., Bianchi, S., Falocco, S., Maiolino, R., Reeves, J. N., & Zappacosta, L., 2005, *A&A*, 435, 867
- Miniutti, G., & Fabian, A. C., 2004, *MNRAS*, 349, 1435
- Nandra, K., George, I. M., Mushotzky, R. F., Turner, T. J., & Yaqoob, T., 1997, *ApJ*, 477, 602
- Petrucci, P. O., & Henri, G., 1997, *A&A*, 326, 99
- Porquet, D., & Reeves, J. N., 2003, *A&A*, 408, 119
- Reeves, J. N., Turner, M. J. L., Pounds, K. A., O'Brien, P. T., Boller, T., Ferrando, P., Kendziorra, E., & Vercellone, S., 2001, *A&A*, 365, L134
- Streblyanska, A., Hasinger, G., Finoguenov, A., Barcons, X., Mateos, S., & Fabian, A. C., 2005, *A&A*, 432, 395